Ueli Angst

Chloride induced reinforcement corrosion in concrete

Concept of critical chloride content – methods and mechanisms

Thesis for the degree of Philosophiae Doctor

Trondheim, January 2011

Norwegian University of Science and Technology
Faculty of Engineering Science and Technology
Department of Structural Engineering

NTNU – Trondheim
Norwegian University of
Science and Technology

NTNU
Norwegian University of Science and Technology

Thesis for the degree of Philosophiae Doctor

Faculty of Engineering Science and Technology
Department of Structural Engineering

ISBN 978-82-471-2762-9 (printed ver.)
ISBN 978-82-471-2763-6 (electronic ver.)
ISSN 1503-8181

Doctoral theses at NTNU, 2011:113

Printed by NTNU-trykk

PREFACE

This doctoral thesis is submitted to the Norwegian University of Science and Technology (NTNU) for the degree of Philosophiae Doctor (PhD). The major part of the work was carried out at the Department of Structural Engineering, Faculty of Engineering Science and Technology at NTNU in Trondheim, Norway; a minor part was carried out at the Institute for Building Materials of the Department of Civil, Environmental and Geomatic Engineering at the Swiss Federal Institute of Technology (ETH) in Zurich, Switzerland.

Main supervisor has been Professor Øystein Vennesland (NTNU); co-supervisors have been Dr. Claus K. Larsen (Norwegian Public Roads Administration/Statens Vegvesen, Oslo, Norway) and Professor Dr. Bernhard Elsener (ETH Zurich, Switzerland).

The project started in April 2007 and completed for submission in January 2011, including approximately one year of duty work as a scientific assistant at the Department of Structural Engineering, NTNU.

The project was part of the Norwegian Concrete Innovation centre (COIN), one of the presently 14 Centres for Research based Innovation (CRI), initiated by the Research Council of Norway. The vision of COIN is creation of more attractive concrete constructions, which – amongst others – includes durability and cost efficiency during the service life. COIN is financed by the Research Council of Norway, industrial partners and by NTNU and SINTEF. For more information, please visit http://www.coinweb.no.

The author, Ueli Angst, declares that this thesis and the work presented in it are his own and have been generated by him as the result of original research while in candidature for the degree of Philosophiae Doctor at NTNU. The thesis contains no material that was previously submitted for a degree at this university or any other institution.

ACKNOWLEDGEMENTS

The Concrete Innovation Centre (COIN) – funded by the Research Council of Norway, industrial partners and by NTNU and SINTEF – is acknowledged for financing this work. The additional financial support from NTNU and the Norwegian Public Roads Administration (Statens Vegvesen) for laboratory measurement equipment is also greatly appreciated.

Many people have contributed to this thesis. First of all, I would like to thank my main supervisor, Øystein Vennesland, for giving me the opportunity to study in Norway, for his support through all stages of this project, and for establishing contact to leading researchers in our research field from all over the world. I would also like to express special thanks to my co-supervisors Bernhard Elsener, for sharing his profound knowledge and providing guidance and many inspiring inputs to my research, and Claus Kenneth Larsen for many valuable discussions and asking myriads of critical questions.

I am also grateful to Roar Myrdal and Anders Rønnquist for their helpful contributions in the fields of electrochemistry and probabilistic safety engineering, respectively, and to Erik J. Sellevold, Mette R. Geiker, and Odd E. Gjørv for many interesting discussions on concrete and durability related issues. The laboratory staff of the Department of Structural Engineering at NTNU is also greatly acknowledged, in particular Ove Loraas and Steinar Seehuus for their assistance in the concrete laboratory and their creative help with all kind of technical problems, and the former employee Andreas Gurk for programming part of the data loggers. Further thanks are due to Jan Eri from Protector AS for his fast and competent support when I was struggling with the Camur II data logging system. I would also like to thank Tone A. Østnor, Kristin Mjøen and all the other people from SINTEF involved in the chloride analyses. Furthermore, many thanks are due to Gabriele Peschke from the Institute for Building Materials at ETH Zurich and Morten Peder Raanes from the Department of Materials Science and Engineering at NTNU Trondheim for their help with scanning electron microscopy and X-ray microanalysis techniques.

I would also like to thank all the colleagues at the Department of Structural Engineering at NTNU for creating a nice working environment.

Last but not least, I wish to express my gratitude to my family in Switzerland, and in particular to my supportive and patient wife Vanessa and my lovely daughter Elin Hanna for giving me the things that are so much more important in life than the combination of chlorides, reinforcement steel and concrete.

SUMMARY

Chloride induced reinforcement corrosion is widely accepted to be the most frequent mechanism causing premature degradation of reinforced concrete structures. Condition assessment and service life prediction is based on comparing the chloride content in the concrete at the steel depth – either measured in the field or computed by means of theoretical modelling – with the chloride content that is believed to be tolerable before corrosion starts. The latter is commonly referred to as *critical chloride content* or *chloride threshold value*. Owing to the considerable statistical variation of the parameters involved in service life considerations, probabilistic approaches are preferentially used since these aim at taking into account the uncertainties inherent to all parameters – at least on a theoretical basis.

The present thesis approached the issue of chloride induced reinforcement corrosion from various angles. First, a non-destructive chloride measurement technique was studied. Second, the critical chloride content was reviewed with particular focus on how to determine this value experimentally and on common practice of its application. In a third part, the mechanism of chloride induced corrosion was experimentally studied.

Regarding the measurement of chlorides, the application of ion selective electrodes (ISEs) as non-destructive chloride sensors in concrete was investigated. It was found that silver / silver chloride electrodes respond to the chloride ion activity in the pore solution as expected from theory and are functional also in highly alkaline environments. However, correct measurement of the sensor potential is the critical step and in this regard, the presence of diffusion potentials was identified as serious error source. These disturbing potentials arise from concentration gradients along the measurement path between reference electrode and ISE, particularly owing to pH gradients and chloride profiles. The error can be minimised by optimal placing of the reference electrode with respect to the ISE. Generally, in uncarbonated, alkaline concrete, the accuracy of this non-destructive chloride measurement method was found to be comparable to the accuracy of common procedures to determine the acid-soluble chloride content in concrete powder. On the other hand, when the pH of the concrete is on a lower level such as owing to the presence of pozzolanas, the adverse effect of diffusion potentials arising from chloride profiles increases and negatively affects the measurement accuracy.

A review on the critical chloride content has shown that this parameter scatters significantly in the literature and that the published data does not offer a basis to improve service life predictions. The reported values are not consistent, particularly regarding non-traditional binder types. This was, at least partly, explained by the wide variety of experimental methods and the pronounced effect of certain experimental parameters. It was concluded that there is a strong need for a generally accepted, practice-related test setup for the critical chloride content. Without reliable input data, the common practice of probabilistic service life modelling is highly questionable. Both based on experimental results as well as the literature review, recommendations were made for a realistic test setup; these include the use of ribbed steel in as-received condition, chloride exposure by cyclic wetting and drying as well as leaving the rebar at its free corrosion potential rather than subjecting it to potentiostatic control.

While it was from experimental work concluded that even in rather small laboratory specimens, the cathode is sufficiently large to provide realistic conditions for (early) pitting corrosion, probabilistic considerations have illustrated that the specimen size is likely to significantly influence the measured critical chloride content. More specifically, the smaller the specimens, the higher the expected mean critical chloride content and the larger the scatter of measured values. It was further discussed how the size effect influences the concept of critical chloride content and service life modelling in general. It was suggested that the size of specimens on which the critical chloride content is measured has to be taken into account when transferring the values to structures of real-life dimensions in probabilistic service life calculations. A procedure of how this can be done by considering structural behaviour was sketched (characteristic length).

Regarding corrosion performance, the steel/concrete interface was found to be the most important influencing factor. Investigations by means of scanning electron microscopy revealed microstructural differences of top and lower sides of rebars that were horizontally orientated during casting, in particular the presence of a bleed-water zone below the reinforcement. It was striking that chloride induced corrosion initiated preferentially on the rebar side with the bleed-water zone regardless of the direction of chloride ingress. Also entrapped air voids were frequently observed at the steel/concrete interface; however, these coincided never with the location of corrosion onset. It was suggested that the internal moisture state is decisive in determining which interfacial defects present a risk of corrosion initiation.

Last but not least, it was experimentally observed that steel embedded in concrete might depassivate/repassivate several times until stable pitting corrosion is achieved – at least under unpolarised conditions. After the first signs of corrosion onset, a marked increase in chloride content was often required to prevent repassivation and to enable stable pit growth. The time at which the chloride content is measured and taken as critical chloride content is thus decisive for the outcome of a laboratory test method. It was suggested that in order to obtain practice-related chloride threshold values, this should be done as soon as stable pit growth is achieved (rather than at the first depassivation event).

Finally, measurements after depassivation provided insight into the mechanism of early pitting corrosion and lead to the conclusion that the corrosion kinetics are at this stage dominated by anodic diffusion control.

TABLE OF CONTENTS

LIST OF PAPERS

This thesis includes the following ten appended papers. They are referred to by their Roman numbers.

I **Potentiometric determination of the chloride ion activity in cement based materials**
U. Angst, B. Elsener, C.K. Larsen, and Ø. Vennesland
Journal of Applied Electrochemistry 40 (2010) 561–573

II **Diffusion potentials as source of error in electrochemical measurements in concrete**
U. Angst, Ø. Vennesland, and R. Myrdal
Materials and Structures 42 (2009) 365–375

III **Detecting critical chloride content in concrete using embedded ion selective electrodes – effect of liquid junction and membrane potentials**
U. Angst and Ø. Vennesland
Materials and Corrosion 60 (2009) 638–643

IV **Diffusion potentials in porous mortar in a moisture state below saturation**
U. Angst, B. Elsener, R. Myrdal, and Ø. Vennesland
Electrochimica Acta 55 (2010) 8545–8555

V **Critical chloride content in reinforced concrete – A review**
U. Angst, B. Elsener, C.K. Larsen, and Ø. Vennesland
Cement and Concrete Research 39 (2009) 1122–1138

VI **Chloride induced reinforcement corrosion: electrochemical monitoring of initiation stage and chloride threshold values**
U. Angst, B. Elsener, C.K. Larsen, and Ø. Vennesland
Corrosion Science 53 (2011) 1451–1464

VII **Probabilistic considerations on the effect of specimen size on the critical chloride content in reinforced concrete**
U. Angst, A. Rønnquist, B. Elsener, C.K. Larsen, and Ø. Vennesland
Corrosion Science 53 (2011) 177–187

VIII Influence of casting direction on chloride-induced rebar corrosion

U. Angst, B. Elsener, C.K. Larsen, and Ø. Vennesland
In: Proceedings of CONSEC'10. *Concrete under Severe Conditions, Environment and Loading, Vol. 1.* Eds: P. Castro-Borges et al., Taylor & Francis, 2010, pp. 359–366.
ISBN 978-0-415-59316-8.

IX Defects at the steel/concrete interface and their influence on chloride induced reinforcement corrosion

U. Angst, B. Elsener, C.K. Larsen, and Ø. Vennesland
Cement and Concrete Research (submitted)

X Chloride induced reinforcement corrosion: rate limiting step of early pitting corrosion

U. Angst, B. Elsener, C.K. Larsen, and Ø. Vennesland
Electrochimica Acta (submitted)

Declaration of authorship for papers I–X

Ueli Angst planned and conducted the major part of the experiments, did the numerical simulations, evaluated the results, and wrote the appended papers. In general the co-authors contributed with constructive criticism that increased the scientific quality of the publications.

As specific additional contributions, Ø. Vennesland, C. K. Larsen, and B. Elsener were involved in planning the experiments for paper I (calibration of ISEs in solution and mortar) and in designing the specimens and the setup that formed a basis for papers VI, VIII, IX, and partly for paper X. During a stay at ETH Zurich in September 2010, B. Elsener gave helpful guidance for evaluation and discussion of the results in papers VI and X. Some of the ideas presented in paper VII, particularly the structural considerations, evolved from discussions with A. Rønnquist.

Ueli Angst performed the major part of the experimental work with exception of chemical analyses (all measurements of chloride content in concrete powder (SINTEF Building and Infrastructure, Trondheim); pore solution composition analysis (preBIO, Namsos) in paper IV), and scanning electron microscopy and X-ray microanalysis in papers I and IX (technical assistance by NTNU Trondheim and ETH Zurich).

OTHER PUBLICATIONS

In addition to papers I–X, the following publications resulted from the work carried out in the present PhD project. These publications are not appended to the present thesis.

Journal papers

- U. Angst. A discussion of the paper "Influence of surface charge on ingress of chloride ion in hardened pastes" by Y. Elakneswaran, T. Nawa, and K. Kurumisawa. *Materials and Structures* 44 (2011) 1–3.

Book chapter

- M.C. Alonso, U. Angst, M. Sanchez, and K.Y. Ann. Onset of chloride induced reinforcement corrosion. In: Handbook of concrete durability. Ed: S.-H. Kim, K.Y. Ann. Middleton Publishing Inc. (2010), ISBN 351-2010-000013, pp. 1–48.

Conference papers

- U. Angst, B. Elsener, C.K. Larsen, and Ø. Vennesland. Considerations on the effect of sample size for the critical chloride content in concrete. In: Service Life Design for Infrastructure, Proc. 2nd Int. Symp., Delft, The Netherlands. Volume 1. Ed: K. van Breugel et al. RILEM Publications S.A.R.L., 2010, pp. 569–576.
  ISBN 978-2-35158-113-1.

- U. Angst, C.K. Larsen, Ø. Vennesland, and B. Elsener. Monitoring the chloride concentration in the concrete pore solution by means of direct potentiometry. In: Concrete Solutions, Proc. Int. Conf. on Concrete Solutions, Padua, Italy. CRC Press/Balkema, The Netherlands, 2009, p. 401.
  ISBN 978-0-415-55082-6.

- U. Angst and Ø. Vennesland. Critical chloride content in reinforced concrete – state of the art. In: Concrete Repair, Rehabilitation and Retrofitting II. Proc. 2nd Int. Conf. on Concrete Repair, Rehabilitation and Retrofitting (ICCRRR), Cape Town, South Africa. CRC Press/Balkema, The Netherlands, 2008, p. 149.
  ISBN 978-0-415-46850-3.

- U. Angst, Ø. Vennesland, C.K. Larsen, and B. Elsener. Critical chloride content for corrosion in reinforced concrete. In: Nordic Concrete Research, Proceedings 20th NCR meeting, Bålsta, Sweden. Norsk Betongforening, Oslo, 2008, p. 52.
  ISBN 978-82-8208-007-1.

SYMBOLS AND ABBREVIATIONS

Symbol	Meaning	Usual dimensions
α	Degree of hydration	–
β_a	Slope of anodic polarisation curve (Tafel slope)	V
β_c	Slope cathodic polarisation curve (Tafel slope)	V
C_{crit}	Critical chloride content, chloride threshold value	% by cement weight
CE	Counter electrode	
CSH	Calcium silicate hydrates	
DCS	Degree of capillary saturation	%
E	Electrochemical potential	V
E^o	Standard electrode potential	V
E_{corr}	Corrosion potential or open circuit potential	V
EDS	Energy-dispersive spectrometer	
EIS	Electrochemical impedance spectroscopy	
ESEM	Environmental scanning electron microscopy	
FA	Fly ash, fuel ash	
F	Faraday constant	96 485 C
GGBS	Ground granulated blastfurnace slag	
I_{corr}	Corrosion current	A
i_{corr}	Corrosion current density (corrosion rate)	A m^{-2}
ISE	Ion selective electrode	
ITZ	Interfacial transition zone	
LOI	Loss on ignition	weight-%
LPR	Linear polarisation resistance	
n	number of electrons in an electrochemical reaction	
n	age factor	–
ρ	Electrical resistivity	Ω m
R	Electrical (ohmic) resistance	Ω
R	Molar gas constant	8.314 J mol^{-1} K^{-1}

Symbol	Meaning	Usual dimensions
R_p	Polarisation resistance or specific polarisation resistance	Ω or Ω m²
RE	Reference electrode	
RH	Relative humidity	%
SCE	Saturated calomel electrode (reference electrode) ca. +244 mV vs. standard hydrogen electrode	
SF	Silica fume	
SHE	Standard hydrogen electrode	
SEM	Scanning electron microscopy	
T	Temperature	K
w/c	Water/cement ratio	–
w/b	Water/binder ratio	–
WE	Working electrode	
Z	Impedance	Ω

These symbols are used in the following chapters and in most of the appended papers. However, in some cases other symbols were used in accordance with the scientific style of the respective journal.

1 INTRODUCTION

Reinforced concrete is one of the most common materials used by the construction industry all over the world. The raw materials required for its fabrication are widely available and the built structures are, in general, durable. Reinforced concrete is used for the construction of transportation infrastructure such as bridges, tunnels, parking garages, retaining walls or harbour structures; it is also used for offshore platforms, dams and a wide range of public and private buildings. Owing to the wide variety of applications, reinforced concrete structures are subjected to a range of exposure conditions, including marine, industrial or other severe environments.

The functionality and reliability of infrastructure is crucial for a society and its economy to function. For the majority of built infrastructure, this is normally the case. However, as an example, according to the annual bridge inventory 2010 [1], approximately 23% of the in total ca. 600'000 bridges in the United States are considered structurally deficient or functionally obsolete. This rating includes all types of bridges (concrete, steel, etc) and apart from corrosion many other causes for structural deficiency and functional obsolescence. Approximately 10 years earlier, the estimated amount of deficient bridges was only about 15%; nevertheless, at that time, the average annual cost to repair and replace US highway bridges specifically owing to corrosion damage was estimated at more than $8 billion (for both reinforced/prestressed concrete bridges and steel bridges) [2]. An even more interesting estimate made in the report was that the indirect costs to the user, and thus the society, due to traffic delays and lost productivity is more than ten times this figure.

Although reinforced concrete might also deteriorate because of alkali silica reactions, freezing-thawing, sulphate or acid attack, it is widely accepted that reinforcement corrosion is by far the most frequent deterioration mechanism. The two main causes for corrosion of steel in concrete are carbonation and contamination of the concrete with chloride. Carbonation describes the process of loss of alkalinity of the concrete owing to the reaction of the alkaline constituents with carbon dioxide of the environment. Chlorides may be present in the fresh mix when using chloride-contaminated materials for the production of concrete (e.g. sea-dredged aggregates or chloride in the cement), but they can also penetrate into the hardened material at a later stage, for instance when exposed to seawater or deicing salt (typically sodium or calcium chloride). Both carbonation and chlorides can lead to breakdown of steel passivity and thus present a risk of loss of rebar cross section and spalling of the concrete cover owing to corrosion. This will affect both serviceability and safety (load bearing capacity) of the structure.

Chloride induced reinforcement corrosion

In the present thesis, only chloride induced reinforcement corrosion is considered. For Norwegian conditions, having a coastline of 25'148 km (including mainland, fjords, islands, etc) [3], where a large number of structures such as harbours and bridges are exposed to marine environment, this is the major cause of reinforcement corrosion. In addition, harsh winters and thus heavy use of deicing salts present a risk of chloride induced corrosion also inland. The same is true for many other countries where road salt is used during winter season.

In Switzerland, for instance, the salt usage during an average winter season is 8–40 tons per kilometre highway, which corresponds to ca. 0.4–2 kg/m² (salt per road surface) [4]. In Alpine regions, the salt load might locally be even higher and during a harsh winter approach 5 kg/m² [5]. According to the US Federal Highway Administration [6], more than 70% of the roads in the United States are located in snowy regions. In the early 1990s, the costs for protection and repair of reinforced concrete structures – specifically resulting from usage of deicing salt during winter – was estimated at $125–325 millions/year for bridge decks and $75–175 millions/year for parking garages, respectively [7]. It was also stated in this report that since the 1960s, when the use of deicing salt became common, this caused more premature bridge deck deterioration than any other damage mechanism.

Having recognised the corrosion risk presented by chlorides, modern standards impose restrictions for the fresh concrete mix by limiting the amount of chloride allowed in the cement (<0.1 weight-% according to EN 197-1 [8]) and in the manufactured concrete (0.2–0.4% by cement weight according to EN 206-1 [9]). Furthermore, the European standard EN 206-1 classifies the exposure conditions by distinguishing chlorides from seawater (XS1, XS2, XS3) and chlorides from other sources such as road salt (XD1, XD2, XD3) where the numbers indicate increasing severity in exposure conditions. Based on these exposure classes, recommendations are given in EN 206-1 for concrete quality (in terms of maximum w/c ratio, minimum strength class, and minimum cement content). In addition, generally in national annexes and standards, also values for the concrete cover depth are specified in a prescriptive manner. Both better concrete quality and higher cover depth will prolong the time required for penetrating chlorides to arrive at the steel surface. This prescriptive approach according to EN 206-1 is intended to ensure a working life of 50 years. It is important to recognise that these recommendations are only valid for Portland cement (CEM I).

Implications of modern binder types

On a world-wide basis, however, the use of CEM I is declining and blended or composite cements are more and more often used instead. One reason for this is the fact that replacement of Portland cement with other mineral additions allows reducing the CO_2 emissions caused by the cement industry. Numerous attempts to develop binders containing significant proportions of non-Portland cement components are thus undertaken. Also within the Norwegian COIN project such research efforts are made, e.g. the development of a composite Portland cement containing fly ash and limestone powder [10].

Since the prescriptions of standards such as EN 206-1 are not applicable to binders other than CEM I, it has during the last years become increasingly popular to use performance based durability design and probabilistic or deterministic service life modelling. These approaches for durability design commonly make use of chloride ingress models to predict the chloride content at the steel surface (cover depth) over time and compare it with the critical chloride content. As soon as the predicted chloride content at the steel surface exceeds the critical chloride content, corrosion is considered to initiate, which generally defines the end of a service life calculation. The parameters that are varied in the calculations in the sense of a trade-off are cover depth and chloride diffusivity (concrete permeability). In contrast to the conventional prescriptive deemed-to-satisfy approach, performance based durability design is thus based on

specifying for instance a maximum chloride diffusion coefficient instead of limiting w/c ratio and minimum cement content.

Another reason for consulting engineers using service life models rather than the prescriptions given in codes, is the fact that public owners occasionally wish their structures to be designed for service lives well exceeding the 50 year time span of EN 206-1. On occasion of the recent international symposium on service life design for infrastructure [11], held in Delft, the Netherlands, numerous presentations were given showing examples of durability design calculations aiming at several hundreds of years of service life.

The modelling approach is recognised to be parameter sensitive particularly in two aspects: Firstly, the time-dependency of the diffusion coefficient, and secondly, the value of the critical chloride content. It might at this point be mentioned that most of today's experience regarding durability performance of reinforced concrete is based on structures built with Portland cement. In addition, having in mind that using reinforced concrete as a construction material started on a serious scale 100–150 years ago, the acquired experience is likely to be insufficient for being extrapolated several hundreds of years into the future. With respect to non-traditional binders, obviously, no long-term experience is available and the implications on the critical chloride content and on the evolution of diffusion properties are unknown. Against this background, it is evident that service life predictions for modern construction materials can at present not be made with a reasonable level of confidence.

While well-established test methods for measurement of the chloride penetration resistance (diffusion coefficient) are available, e.g. Refs. [12-13], and thus in principle allow studying the effects of binder type on diffusion properties, this is not the case for the critical chloride content. It is thus widely recognised that there is an urgent need for a practice-related, standardised – or at least "generally accepted" – test-setup to measure the critical chloride content. This is also highlighted by the RILEM committee "corrosion initiating chloride threshold concentrations in concrete" [14], that was recently initiated and aims at providing recommendations for such a test method.

A final comment is to be made on the propagation stage, viz. the part of service life after corrosion initiation. Several parameters such as temperature, moisture conditions or electrical concrete resistivity are known to affect the rate of corrosion propagation. Depending on these factors, decades might pass after corrosion initiation without losing significant rebar cross section and thus load bearing capacity. Conventional service life models do not take into account this so-called propagation stage, i.e. the service life is considered ended at the time of corrosion initiation. To allow holistic assessment of use of modern binders regarding chloride induced corrosion, both the implications on the initiation as well as the propagation stage should thus be considered. Substantial research efforts are, however, still required until this will be possible in a transparent and reliable manner.

The present thesis approaches the topic of chloride induced reinforcement corrosion from several angles. It is evident that in order to study chloride induced reinforcement corrosion in concrete, techniques to measure the chloride content are highly relevant. Thus, a non-destructive technique to monitor the free chloride ion concentration in the pore solution is studied. Furthermore, the concept of critical chloride content is thoroughly reviewed. Focal points are the effects of experimental parameters with respect to a test setup suitable to provide

realistic data. In this regard, factors such as specimen size, casting direction, and electrochemical techniques are discussed. Not only the experimental methodology with which the critical chloride content is measured, but also the way the laboratory results are treated and applied to practical situations is believed to be decisive when aiming at reliable service life predictions. Finally, the early stage of corrosion propagation is studied by experimental means and discussed with regard to the factors controlling the corrosion rate.

2 OBJECTIVES AND LIMITATIONS

It was the aim to approach the topic of chloride induced reinforcement corrosion by studying the following three points:

1. **Measuring the free chloride ion concentration in the concrete pore solution**

   Improve the non-destructive measurement method based on ion selective electrodes (direct potentiometry) to determine the free chloride ion concentration in concrete. This involves identification of main error sources as well as understanding and quantification of their effect on the measurement results.

2. **Concept of critical chloride content**

   Review the critical chloride content (chloride threshold value) with particular focus on how to determine this parameter experimentally (test methods) and on common practice of its application (concept of C_{crit}). Derive a laboratory test setup that is expected to give practice-related results.

3. **Mechanism of chloride induced corrosion**

   Use the experimental setup that evolves from objective no. 2 in order to study the mechanism of chloride induced reinforcement corrosion.

The exposure conditions considered in the present work are concrete members situated in the splash zone of marine environment or road salt and thus represent aerated rather than continuously submerged concrete. Only chloride induced reinforcement corrosion is considered; the effect of carbonation is neglected. It is not aimed at studying countermeasures against chloride induced corrosion, such as stainless steel, surface coatings, or electrochemical treatments to prolong service life. Neither is it aimed at providing input data for service life models, e.g. values for the parameter *critical chloride content*.

3 THEORETICAL BACKGROUND

3.1 Fundamentals of steel reinforcement corrosion

Corrosion process

Reinforcement steel is an alloy that essentially consists of iron and a comparatively small amount of carbon. In nature, most of the iron exists in a stable state as iron ore, mainly oxides such as magnetite (Fe_3O_4) and hematite (Fe_2O_3) [15]. For the production of steel, energy is required at the steel mill to transform iron ore into steel. The process of *metallic corrosion* can be regarded as the tendency of converting the manufactured construction material back to the original state. The products that thereby form are iron oxides or hydroxides and are commonly referred to as *rust*. Metallic corrosion is normally regarded as an undesirable process of deterioration.

The conversion of iron or steel into rust is electrochemical in nature, viz. the electrochemical reactions – as distinguished from chemical reactions – involve the passage of electrical charge. Electrons are released in the oxidation reaction, and consumed in the reduction reaction. For steel in neutral to alkaline environments, the following electrochemical reactions are usually relevant [16]:

Oxidation reaction (dissolution of iron):

$$Fe \rightarrow Fe^{2+} + 2e^- \tag{1}$$

Reduction reaction (oxygen reduction):

$$H_2O + \frac{1}{2}O_2 + 2e^- \rightarrow 2OH^- \tag{2}$$

For these two *half-cell reactions* to occur, the presence of water as well as oxygen – the latter dissolved – is required. As accumulation of charge is impossible, the two reactions must occur at the same rate. The overall reaction can be written as follows:

$$Fe + H_2O + \frac{1}{2}O_2 \rightarrow Fe(OH)_2 \tag{3}$$

Under usual conditions of reinforcement steel embedded in concrete, the corrosion product $Fe(OH)_2$ will be further oxidised to Fe_3O_4 or Fe_2O_3 [16].

Electrode potentials

Whenever a metal (electrode) is immersed in a solution, a phase boundary metal/solution is established and metal ions dissolve. Thereby, charge in the form of metal ions is passed into the solution and electrons are left behind. The solution is called *electrolyte* as it contains dissolved metal ions (and probably also other ions), and is thus electrically conductive. An *electrical*

double layer is formed with electrons in the metal and (solvated) metal ions in the electrolyte. The charge separation at the phase boundary gives rise to an electric potential difference across the double layer. This potential depends on the type of metal as well as on the electrolyte and is a measure of the tendency of the metal to ionise, viz. to dissolve into the electrolyte.

The potential of a half-cell reaction, such as the one described by eq. (1), can be measured vs. another half-cell or reference electrode. At standard conditions, these potentials are termed *standard electrode potentials*, usually designated E^o. Standard conditions mean temperature of 25°C, pressure of 1 bar, and concentration of metal ions in the electrolyte of 1 mol/l. For other conditions, e.g. at a different concentration of metal ions in the solution, the electrode potentials change and can be calculated with the *Nernst equation*, for the case of iron and reaction (1):

$$E_{Fe/Fe^{2+}} = E^{o}_{Fe/Fe^{2+}} + \frac{RT}{2F} \ln c(\mathrm{Fe}^{2+}) \tag{4}$$

Here, R is the gas constant, T temperature, F the Faraday constant (see symbols and abbreviations) and $c(\mathrm{Fe}^{2+})$ is the concentration of iron ions in the electrolyte.

Potential-pH diagrams (thermodynamic stability)

In certain electrochemical reactions, hydroxide or hydrogen ions are involved (for instance in eq. (2)). The reactions are thus related to the pH of the electrolyte (solubility products). These chemical equilibrium conditions in combination with the Nernst equation, allow calculating regions of thermodynamic stability in an aqueous environment. Stability can be calculated for both anodic and cathodic charge transfer reactions as well as possible purely chemical

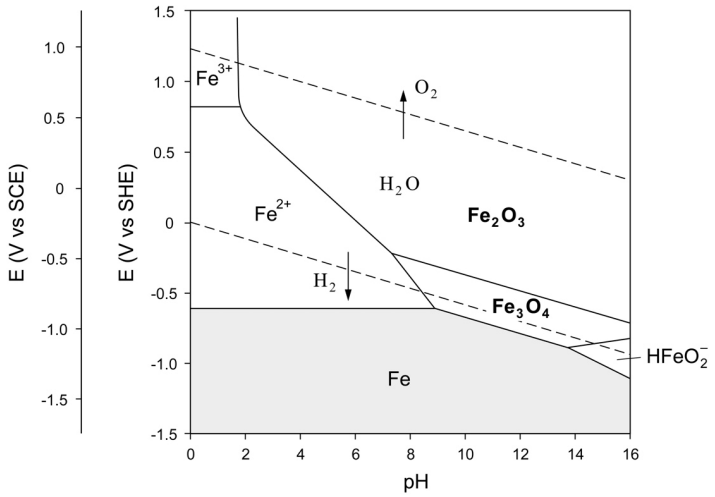

Fig. 1. Pourbaix diagram for iron in water (for ion concentration 10^{-6} mol/l and 25°C). Only Fe, Fe_3O_4, Fe_2O_3 as solid products considered. After Ref. [17].

reactions, as a function of electrode potential, pH and the concentrations of the metal ions in the electrolyte. Such diagrams are also referred to as *Pourbaix diagrams* and can be found for many aqueous electrochemical systems in the literature [17].

Fig. 1 shows regions of stability of iron and its oxides in water. Intermediate products such as $Fe(OH)_2$ are not shown as these oxidise further to Fe_3O_4 and Fe_2O_3. The grey area is termed *immunity* as in this potential/pH range, iron is stable; it will neither dissolve into the electrolyte nor form oxides [16].

The dashed lines represent the hydrogen electrode and oxygen electrode, respectively; between these lines, water is stable and dissociates into H^+ and OH^-. Above the *oxygen line*, it decomposes into O_2; below the *hydrogen line*, evolution of H_2 takes place. For neutral to alkaline environments, decomposition of water into oxygen can be described by eq. (2) when considering that it occurs as an oxidation reaction (it is written as a reduction reaction according to SI rules). Hydrogen evolution occurs as follows:

low pH: $$2H^+ + 2e^- \rightarrow H_2 \quad (5)$$

neutral/alkaline: $$2H_2O + 2e^- \rightarrow H_2 + 2OH^- \quad (6)$$

Note that depending on the species present in the electrolyte, also oxidation and reduction reactions other than the ones depicted in Fig. 1 are possible; the same is true for purely chemical reactions.

Passivity

As apparent from Fig. 1, iron and water are not simultaneously stable regardless of pH (at standard conditions). Unless polarised to a potential negative enough to achieve immunity, iron will thus dissolve (acidic/neutral conditions) or form iron oxides (alkaline conditions). Formation of iron oxides can lead to passivity [16]. In this case, the metal itself is thermodynamically not stable, but covered by a stable, dense, transparent *passive film* of only a few nanometres in thickness. This *passive layer* is able to prevent further dissolution of the underlying metal and thus reduces the corrosion rate to insignificantly low levels.

Pitting corrosion (chloride induced corrosion)

It is well known that halides – particularly chloride owing to its presence in many environments – attack the passive layer and can lead to local breakdown of the protective oxide film [18-20]. In contrast to general corrosion where the corrosion attack occurs homogeneously on the entire surface of the metal (e.g. iron in acidic environments, compare Fig. 1), a local damage in the passive film leads to *localised corrosion*. Once a pit, i.e. a small cavity has formed, its geometry imposes restrictions to mass transport. If oxygen diffusion into the pit is slower than its depletion through the cathodic reaction, *deoxygenation* occurs. As a result, oxygen reduction is confined to surfaces adjacent to the pit, while inside the cavity, almost pure

anodic iron dissolution might take place (eq. (1)). To avoid repassivation, the solution inside the pit (anolyte) is required to maintain aggressive chemistry [18,21]. The dissolved iron ions hydrolyse and thereby cause *acidification* of the anolyte to occur, e.g. by the following chemical reaction [19]:

$$Fe^{2+} + 2H_2O \rightarrow Fe(OH)_2 + 2H^+, \quad (7)$$

or by the electrochemical oxidation reactions [18]:

$$2Fe^{2+} + 3H_2O \rightarrow Fe_2O_3 + 6H^+ + 2e^- \quad (8)$$

$$3Fe^{2+} + 4H_2O \rightarrow Fe_3O_4 + 8H^+ + 2e^- \quad (9)$$

Fig. 2 schematically shows a pit cavity where anodic iron dissolution and subsequent hydrolysis of the iron ions occur. To maintain electroneutrality and balance the positive charge produced in the pit, anions (negatively charged ions) move into the pit and cations (positively charged ions) migrate to the exterior bulk solution. In pure neutral or alkaline water, hydroxide will migrate into the pit and prevent a fall in pH; acidification of the anolyte can thus only occur in the presence of negative ions other than OH^-, such as chloride or sulphate ions [18].

As a result of the deoxygenation-acidification mechanism, a *macro-cell* is established, i.e. the anodic and cathodic half-cell reactions are spatially separated. Anodic iron dissolution preferentially takes place in the acidic deaerated pit environment, while cathodic oxygen reduction proceeds on the alkaline, aerated external metal surfaces. Fig. 2 schematically summarises the localised character of pitting corrosion with the involved charge transfer reactions, mass transport processes and the macro-cell. Inside the pit cavity, cathodic hydrogen evolution according to eq. (5) might also occur [22] (not shown in Fig. 2).

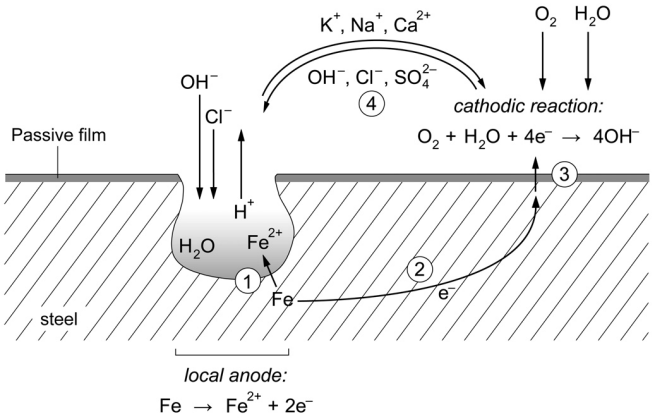

Fig. 2. Schematic illustration of chloride induced pitting corrosion and reaction steps: 1. Anodic iron dissolution; 2. Flow of electrons through metal; 3. Cathodic reduction reaction; 4. Ionic current flow through the electrolyte.

Kinetics

In the established macro-cell, a current is passing through the circuit. Since, according to Kirchhoff's law, there must be continuity in the currents, the following four steps have to take place at the same rate:

- Anodic dissolution of iron and release of electrons according to eq. (1)
- Transport of electrons through the metal from the anodic to the cathodic sites
- Cathodic reactions to consume the electrons; in the case of steel corrosion in concrete mainly oxygen reduction according to eq. (2) is relevant
- Flow of electric current through the electrolyte between anodic and cathodic sites, carried by flux of ions

The current flow through the metal is never rate limiting as steel is highly conductive. Thus, the slowest of the remaining three steps will determine the corrosion rate. Prediction of this is, however, not straightforward, since the rates of the individual steps are not independent of each other.

The flux of electrons in the macro-cell (electrical charge per unit time, ampere (A)) can be regarded as a measure for the *corrosion rate* (as long as only one oxidation reaction occurs).

The rate at which anodic and cathodic reactions occur depends on the electrochemical potential of the Fe/Fe^{2+} and oxygen electrode, respectively. The relationship between potential and current of an electrode is called *polarisation curve*. In general, the corrosion current increases when the anode potential is raised to more positive values; the reaction rate of the cathodic half-cell reaction increases with declining potentials (to more negative values).

In Fig. 3b, polarisation curves for steel in alkaline as well as acidic environment are

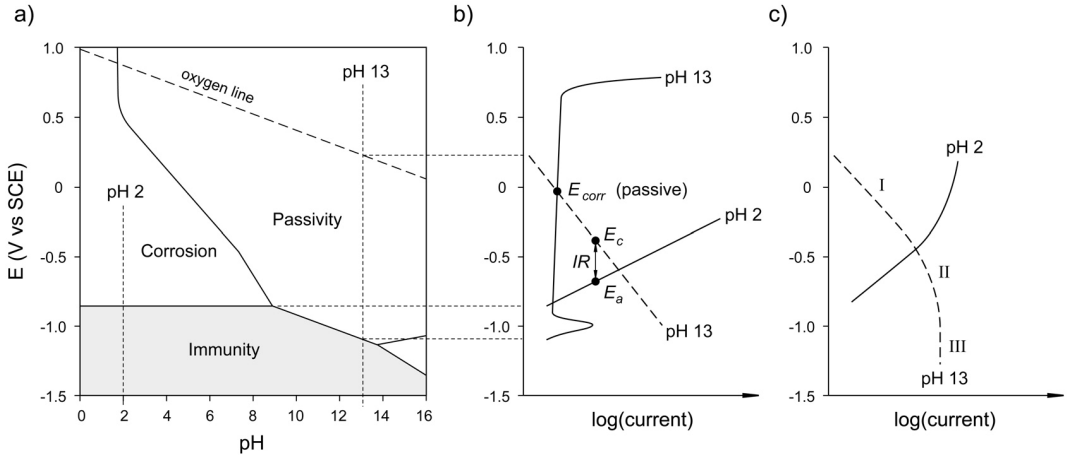

Fig. 3. Simplified Pourbaix diagram for iron (a) and schematic anodic (solid line) and cathodic (dashed line) polarisation curves in active and passive regions (b); effect of diffusion control (c). The ordinate is the same for all three graphs.

schematically depicted and related to the Pourbaix diagram. At high pH, a large range of passivity is visible where the anodic current (iron dissolution) is on a low level, almost independent of potential; at low pH, the logarithm of the anodic current increases linearly with the potential. As the cathodic reaction occurs on metal surfaces outside the pit, the dashed line describing cathode kinetics in Fig. 3b is drawn for high pH. When the potential decreases to more negative values, the logarithm of the cathodic current increases linearly.

Activation control and diffusion control

When the polarisation curves in an *E*-log*I*-diagram are straight lines, the reaction kinetics are said to be purely *activation controlled*. The slope of the line is called *Tafel constant*. For activation controlled reactions, all the involved species have to be readily available at the electrode surface so that the passage of charge across the electrode/electrolyte interface determines the rate (which is a function of potential). For instance, if oxygen reduction according to eq. (2) is to proceed, dissolved oxygen is required at the electrode surface to be consumed at the rate of the cathodic reaction. However, the concentration of oxygen is limited by its solubility. Thus, oxygen might be consumed in the half-cell reaction at a higher rate than the rate at which dissolved oxygen reaches the electrode surface. In this case, mass transport (oxygen diffusion) from the bulk solution to the electrode becomes rate limiting and the process is under so-called *diffusion control*. As mass transfer in the electrolyte is independent of the electrode potential, the polarisation curve becomes a vertical line. Fig. 3c shows a cathodic curve with a purely activation controlled region (I), a transition region (II), and a purely diffusion controlled region (III).

In the case of pitting corrosion, also the anodic reaction kinetics can be under diffusion control, since, as discussed above, maintaining aggressive pit chemistry requires transport of ionic species into the pit (e.g. chloride ions). Particularly at higher corrosion rates, supply of chloride ions to migrate from the bulk solution through the narrow pit mouth to reach the pit bottom might be restricted. This process is governed by the composition of the bulk electrolyte (e.g. chloride concentration) and the pit geometry (e.g. deep and narrow vs. open). An example of an anodic polarisation curve under diffusion control is shown by the solid line in Fig. 3c.

Open circuit potential

As all the electrons liberated in the oxidation reaction have to be consumed in the reduction reaction, the total anodic current has to be equal to the total cathodic current. When the electrode surfaces of anode and cathode have the same size, also the *current densities*, i.e. the current divided by the electrode surface (for instance in $\mu A\ cm^{-2}$), have to be equal. Otherwise, to consider current balance, the current densities have to be multiplied with the respective surface areas to obtain the total anodic and cathodic currents (for instance in μA). In Fig. 3b,c, the abscissa is shown in terms of total current of the reaction rather than current density; thus, an intersection of anodic and cathodic polarisation curves represents a point where the amount of electrons liberated in the oxidation reaction is equal to the amount of electrons consumed in the reduction reaction.

In the passive state, very little iron dissolution takes place and both the anodic and cathodic reactions occur homogeneously over the entire electrode surface. Current balance is obtained at the so-called *open circuit potential* or *corrosion potential*, E_{corr}, as shown in Fig. 3b.

Ohmic drop

In the case of active localised corrosion, the cathode surface is generally much larger than the anode surface and anodic and cathodic sites are spatially separated. The electrical circuit in the macro-cell has to be closed by current flow through the electrolyte (Fig. 2). In the presence of an ohmic resistance against this current flow, the potentials of anode and cathode are not equal. Energy is dissipated by the ionic current passing the resistance in the electrolyte. This voltage drop is usually referred to as *ohmic drop* or *IR drop*. Fig. 3b shows the case of active dissolution in acidic pit environment at the anode potential, E_a, and the cathodic reaction on exterior surfaces (alkaline environment) at the cathode potential, E_c, as well as the *IR* drop in the electrolyte. While the current of the anodic reaction is equal to the one of the cathodic reaction, the potentials are different.

For a metal immersed in aqueous solution, the resistance in the corrosion cell, R, is a function of electrolyte conductivity and geometrical configuration. When charge transfer reactions occur homogeneously over the entire surface, the distance between local anodic and cathodic sites is small and the *IR* drop can be neglected. In this case, anode and cathode are forced to stabilise at the same potential, E_{corr} (e.g. in the passive state).

Evans diagrams

The way of presenting reaction kinetics as in Fig. 3b,c is common in corrosion science. The diagrams are, after their inventor, named *Evans diagrams*. Whereas Pourbaix diagrams depict the thermodynamic stability, viz. which products are stable under certain conditions, and contain no information on kinetics, Evans diagrams visualise the reaction kinetics of an electrochemical system and the involved electrodes as a function of potential.

Rate limiting process

Regarding the current circuit in the macro-cell, it is apparent that both anodic and cathodic reactions as well as the ionic current flow through the electrolyte can be the rate limiting step. When the cathodic reaction is strongly restricted, e.g. by oxygen starvation in a submerged situation, the process is under *cathodic control*. In this case, mass transfer limits the cathodic reaction. Note that the cathode might also be rate limiting without necessarily being under diffusion control, for instance when the cathodic electrode surface is small or the reaction kinetics (activation control) are limited as is the case on certain metal surfaces (high Tafel slope, i.e. a steeper line in Evans diagram).

The anodic reaction might also be the rate limiting step; the process is then under so-called *anodic control*. When the metal is passive, the slope of the anodic polarisation curve is high, almost vertical, and thus determines the reaction rate (Fig. 3b). In an active state, the anodic reaction kinetics might be limited owing to the pit geometry restricting mass transport and thus the mechanism is more specifically termed *anodic diffusion control*.

When the flow of ionic current through the electrolyte (from anodic to cathodic sites) is restricted owing to a high ohmic resistance (low conductivity) and/or the geometrical configuration, the process can be under *ohmic control*.

These rate limiting steps are in more detail discussed in paper X of the present thesis.

3.2 Concrete

Concrete is produced by mixing its main constituents aggregates (sand and gravel), cement and water. Cement chemically reacts with water, a process referred to as cement *hydration*, that leads to hardening of the fresh concrete and finally results in a solid composite material. The product of cement hydration, the so-called *cement paste*, determines most of the properties of hardened concrete. One of the most important parameters in this regard is the ratio of water and cement in the mix (w/c ratio).

Cements and hydration

Various types of cement exist, most of them based on *Portland cement clinker*. It consists to a large extent of tricalcium and dicalcium silicates and to a minor extent of calcium and iron-calcium aluminates, gypsum as well as other minor components such as alkali oxides (Na_2O, K_2O) [23]. When mixed with water, it reacts to *calcium silicate hydrates*, abbreviated as CSH, a gel composed of particles with a layer structure [23]. Another product of Portland cement hydration relevant for the corrosion behaviour of embedded steel is calcium hydroxide ($Ca(OH)_2$).

Certain siliceous materials have the ability to react with water and calcium hydroxide to form calcium silicate hydrates as well. These materials are termed *pozzolanic materials* or *pozzolanas* and the reaction leading to CSH is the so-called *pozzolanic reaction* [23]. If blended with Portland cement, they reduce the content of calcium hydroxide in the hydrated cement paste (as it is consumed in the pozzolanic reaction), but increase the amount of CSH. In addition, during production, they are usually associated with lower energy consumption (as they are waste products from other industrial processes) and/or lower emissions that adversely affect the environment. Pozzolanic materials commonly used in the cement industry to partially replace ordinary Portland cement are fly ash (FA, a bi-product of coal combustion in thermal power plants), condensed silica fume (SF, a waste product of the silicon or ferro-silicon production industry), and natural pozzolanas such as volcanic ashes. In addition to pozzolanic materials, Portland cement is blended with other mineral additions such as ground granulated blast furnace slag (GGBS, a bi-product of the steel industry) or limestone filler. The European standard EN 197-1 [8] distinguishes the following types of cement:

- *Portland cement* (CEM I), with >95% clinker
- *Portland-composite cements* (CEM II) with up to 35% of another single mineral constituent (GGBS, SF, FA, natural pozzolanas, burnt shale, or limestone)
- *Blastfurnace slag cement* (CEM III) with 36–95% GGBS
- *Pozzolanic cement* (CEM IV) with 11–55 % of a pozzolanic material (SF, FA, or natural pozzolanas)
- *Composite cement* (CEM V) with 18–50% GGBS and 18–50% FA or natural pozzolanic material

In addition to blended cements, where binders and mineral additions are blended by the cement producer, pozzolanas (and other mineral additions) might also be added at the concrete plant.

Pore structure

According to the classical theory based on the work by Powers and Brownyard [24], the cement paste formed during cement hydration contains pores, which are considered as the volume that may be occupied by evaporable water. Upon mixing cement and water, the space between the cement particles is initially filled with water, but during hydration, cement hydration products grow and fill the space, thereby reducing the volume of this interconnected capillary system. The volume fraction of the remaining *capillary pores* depends on w/c ratio and the degree of hydration; on a theoretical basis, at low w/c ratios (below ~0.4) and full hydration the capillary porosity is zero. However, when cement reacts with water, the product of the reaction has a smaller volume than the substances before hydration (chemical shrinkage). This difference in volume leads to the formation of pores, which, as long as water and unhydrated cement are present, can fill up with cement hydration products. When cement paste with a w/c ratio below ~0.4 hardens under isolated conditions, viz. no humidity exchange with the environment, the chemical shrinkage pores remain empty owing to lack of water. This volume accounts for capillary porosity. Since in concrete members of practical dimensions, isolated hardening is usually the case in the internal part of the concrete, capillary porosity can practically not be avoided. However, *discontinuity* can be reached, i.e. although capillary pores are present, they are not interconnected. According to Powers et al. [25] capillary discontinuity is achieved after two weeks of hardening for $w/c < 0.5$, requires 6 months for $w/c = 0.6$, and is impossible for $w/c > 0.7$. Nevertheless, the existence of capillary discontinuity has controversially been discussed, e.g. in Refs. [26-27]. In addition, also the theory regarding formation of capillary porosity suggested by Powers and Brownyard [24], as pointed out above, has been questioned in the literature as recently reviewed in Ref. [28].

However, pores ranging in size from a few nanometres to several micrometres are generally considered *capillary pores* [29-31]. Interlayer spaces of the CSH gel, according to Powers et al. [24,32] generally referred to as *gel pores*, are only a few nanometres in size. In addition, *macro pores* or *air voids* exist in concrete owing to entrapped air bubbles or incomplete compaction.

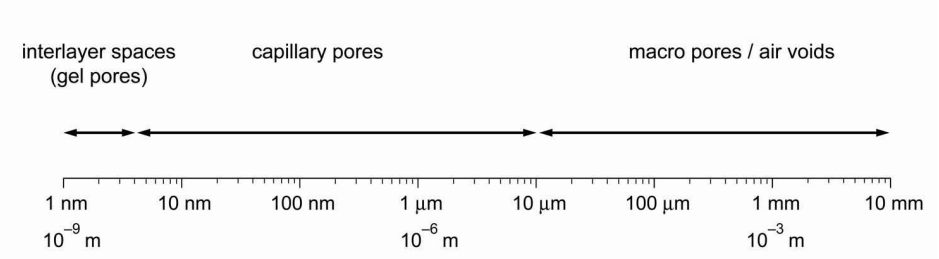

Fig. 4. Range of dimensions of pores in concrete (indicative).

They can have diameters of up to several millimetres [29-31]. In concrete, the largest pores might thus be more than one million times larger than the smallest ones (Fig. 4).

It might be mentioned that the porosity of cement paste differs strongly from the porosity of concrete. One of the reasons for this is the variation in cement paste properties between bulk paste and the zone adjacent to aggregates. In this *interfacial transition zone* (ITZ), the capillary porosity is generally higher with better interconnectivity and also the hydration products are different. More details on properties of this zone are reported in the literature, e.g. in Ref. [33]. A similar ITZ also forms at the interface of reinforcement steel and cement paste and has implications on the corrosion behaviour [34-38] as also discussed in paper IX.

Last but not least, *cracks* are likely to be present in real-world concrete for instance owing to static or dynamic loads or as the result from thermal gradients during the hardening stage (cement hydration heat).

Moisture content

Given the pore structure, water in concrete can be present in different forms [39-40]: chemically bound water (combined in hydration products), interlayer water (held in gel pores), adsorbed water (on the pore walls), capillary water (held in capillaries), and water in macro pores and air voids. The amount of chemically bound water depends on the degree of hydration; at full hydration ($\alpha = 1$) its amount is generally assumed at 0.23–0.25 g water/g cement [24]. Chemically bound water is only released when cement paste is ignited and decomposes (at temperatures up to >1000°C).

Interlayer water, adsorbed water, capillary water, and water in macro pores on the other hand, are evaporable. When water has evaporated from pores, a layer of adsorbed water is present on the pore walls regardless of pore size. The thickness of the adsorbed layer depends on the relative humidity in the pores and the amount of water adsorbed in the pore system of cement paste is proportional to the internal pore surface.

Capillary pores hold water by capillary forces. The radius of capillaries that are stably water-filled depends, among other factors, on temperature and relative humidity of the environment and can be calculated according to capillary condensation theory (Kelvin-Laplace equation, e.g. Ref. [39]). Indicatively, according to this theory, at a temperature of 20°C, the stable radius of a cylindrical pore is in the range 3–10 nm for relative humidities from 70% to 90%.

Macro pores have no capillary action and thus only fill up when the concrete is submerged. This was a relevant aspect for the discussion in papers VIII and IX.

Field measurements have shown that the moisture content in concrete structures exposed in northern Europe coastal climate is ca. 70–80% RH, which corresponds to a degree of capillary saturation (DCS) in the range 75–90% [41].

Permeability and transport properties

The pore structure of concrete is, in principle, permeable. The parameter *concrete permeability*, i.e. the extent to which it permits transport of liquids and gases, is vital for most deterioration processes affecting durability of reinforced concrete [29,40]. Of particular interest in the present thesis is the permeability to chloride dissolved in water.

Aggregates have usually low permeability – with some exceptions (e.g. lightweight aggregates) – and thus transport mechanisms occur essentially through the pore system of the cement paste, the ITZ, and cracks or fissures in the concrete. As gel water and adsorbed water are under the effect of surface forces, they are usually believed not to significantly contribute to transport processes. Transport properties can thus be correlated to the amount of capillary pores and their interconnectivity. This is apparent from Fig. 5a that shows the permeability coefficient for stationary water transport in cement paste vs. the volume fraction of capillary porosity. As discussed above, the pore structure, and in particular the presence of capillaries, strongly depends on w/c ratio and degree of hydration, and thus it would not be surprising if permeability correlated with w/c ratio. Fig. 5b shows that (for hydrated cement paste) this is indeed the case and that permeability increases markedly and non-linearly with increasing w/c ratio, particularly above w/c ≈ 0.5.

Chloride ingress into concrete

It is important to recognise that Fig. 5 is valid for cement paste; for concrete – that also contains aggregates, ITZ and cracks – transport properties and permeability are different. Transport of aggressive ionic species, such as chloride ions, occurs in the water phase, mainly by the following mechanisms: *capillary suction*, *diffusion*, *permeation*, and *migration*.

When concrete comes in contact with water, capillary forces lead to a relatively fast uptake of

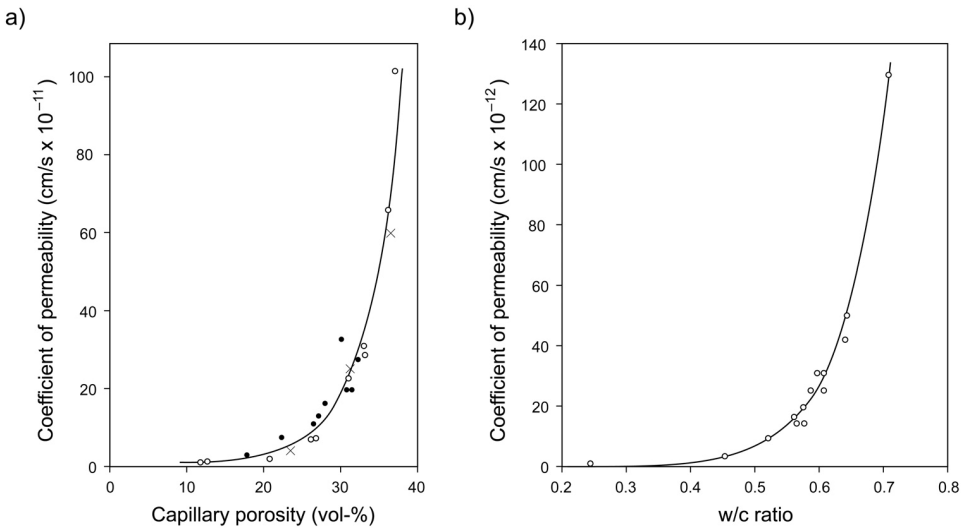

Fig. 5. a) Relationship between water permeability and capillary porosity, according to Powers [42], different symbols represent different cement pastes; b) permeability vs. w/c ratio of mature cement paste (α = 0.93), according to Powers et al. [43].

water. Chloride ingress then happens as the water sucked into the concrete carries dissolved chloride ions. Having in mind the concrete pore structure, this strongly depends on the amount of capillaries as well as their interconnectivity. Capillary suction is usually the dominant mechanism for concrete in the splash zone of, for instance, seawater or salt bearing water on roads [31,40]. During cyclic wetting and drying, capillary water uptake occurs in the wetting stage, while the drying periods allow the capillaries to be, at least partly, emptied, which enhances capillary suction in the next wetting cycle. Note, however, that water absorption by capillary action occurs considerably faster than water loss by evaporation during the drying cycles [39-40].

In the case of water-saturated concrete, e.g. for submerged structural members, diffusion is the main transport process. Permeation, induced by hydraulic pressures, might also play a role. The driving force for diffusion of dissolved species, such as oxygen or chloride ions, is the presence of concentration gradients. For non-stationary conditions, i.e. when the concentration gradient changes with time, the flux can be described by *Fick's second law of diffusion*, which is a mass balance equation (in 1-dimensional notation):

$$\frac{\partial c}{\partial t} = D\frac{\partial^2 c}{\partial x^2} \tag{10}$$

Here, c is the concentration, t the time, x the coordinate, and D the diffusion coefficient. The latter depends on the diffusing species and the concrete microstructure.

The depth to which capillary suction influences the moisture state in concrete is limited. One reason for this is the limited interconnectivity of the capillary pore system. Thus, for structures in the splash zone, a combination of capillary suction (in the outermost millimetres or centimetres of the concrete cover) and diffusion (at deeper distances from the surface) dominates the ingress of species dissolved in the water. Capillary suction is in general regarded as a much more efficient transport mechanism than diffusion since the chloride ions are carried with moving water rather than diffusing in static water. This requires, however, the presence of sufficient interconnected capillary porosity.

Migration, or electromigration, of ions occurs in the presence of an electric field. The velocity of the migrating ions depends on the ionic mobility and the strength of the electric field [44]. In reinforced concrete, electric fields can be present when electrochemical techniques such as cathodic protection are applied, when macro-cells are established in the case of localised corrosion (section 3.1), or when different ionic species diffuse so that diffusion potentials arise as is discussed in more detail in papers II–IV of the present thesis.

Durability aspects

Regarding durability, several parameters are commonly used to characterise the concrete properties with respect to ingress of aggressive species. These include permeability (water transport under hydrostatic pressure), porosity and pore size distribution (determined by absorption techniques, mercury intrusion porosimetry, etc), ion diffusivities (from diffusion or migration cell experiments), or electrical resistivity. Although various procedures and methods exist to determine these variables, and although the variables do not directly represent the same properties, the results are generally in agreement on a qualitative level. Low permeability,

low porosity (in particular low capillary porosity), low diffusivity, and high electrical resistivity are beneficial with respect to durability since this indicates slower penetration of aggressive species.

There is a general consensus that in the case of blended cements, hydration of pozzolanic materials and of blastfurnace slag, lead to a denser microstructure compared with the one obtained from hydration of pure Portland cement [23]. Particularly on the long-term, these reactions refine the pore structure, viz. the amount of larger capillary pores is reduced and more fine pores are formed instead. As a result, the pore structure becomes more impervious.

3.3 Steel embedded in concrete

This section discusses how the corrosion principles presented in section 3.1 are affected for the specific case of reinforcement steel embedded in concrete.

Alkaline environment and passivity

Section 3.2 has shown that in usual environmental conditions concrete holds water in the pore system. The chemistry of this water, in the following referred to as *concrete pore solution*, depends to a large extent on the cement hydration products in the concrete as these are in equilibrium with the pore solution. Owing to the presence of $Ca(OH)_2$ as well as alkali metal ions Na^+ and K^+, the alkalinity is generally high. Pore solution compositions of uncarbonated, seld-desiccated mortar with Norwegian CEM I, reported in paper IV, show that the pH is between 13.5 and 13.7. These values are in agreement with pH values in the literature, which generally lie in the range pH 13–14, e.g. Refs. [45-49].

Thanks to the high alkalinity, steel is able to passivate (Fig. 1). The passive film is stable as long as the pH remains on a high level, according to Fig. 1 above pH~9. The alkalinity of concrete pore solution might be affected by leaching, e.g. in the outer cover zone exposed to rain, or carbonation, i.e. the reaction of calcium hydroxide with CO_2 from the environment. In addition, the pH declines in the presence of pozzolanic minerals owing to the pozzolanic reaction (section 3.2), which has well been documented in the literature [45,50-54]. Although the pH is in the presence of pozzolanas generally not reduced to levels that render the formation of the passive layer impossible, the resistance against loss of alkalinity owing to interaction with the environment is smaller when using pozzolanas.

In atmospherically exposed concrete, oxygen reduction according to eq. (2) is the relevant reduction reaction. For passive steel, as the passive current density is very low, the corrosion potential is close to the reversible potential of the oxygen reduction reaction (Fig. 3b). The latter is a function of pH as apparent from Fig. 1, and of oxygen concentration. In alkaline, aerated concrete, corrosion potentials in the passive state are usually in the range of −200 to +100 mV SCE; for submerged structural members, where oxygen gets depleted, much lower potentials can occur in the passive state [31].

Critical chloride content or chloride threshold value

Passive steel in concrete might in the presence of chloride suffer from localised corrosion. The chloride concentration required to destroy the passive film of steel embedded in concrete is termed *critical chloride content* or *chloride threshold value*, abbreviated C_{crit}. It depends on many factors, as in detail reviewed in paper V of the present thesis, and will thus only briefly be discussed here. A vital parameter for C_{crit} is the pH of the pore solution, since in the presence of hydroxide ions, the amount of chloride ions required for corrosion initiation increases. Probably the most famous reference in this regard is the one by Hausmann [55], that suggested a critical ratio of chloride and hydroxide ions of $Cl^-/OH^- = 0.6$; in other words, when the pH is

as an example 13 instead of 12, the tolerable chloride ion concentration is ten times higher than at pH 12. The high alkalinity of concrete pore solution – markedly above the pH required for iron passivation (Fig. 1) – is thus a major reason for the resistance against chloride induced corrosion. This has to be born in mind when reducing the pH owing to use of pozzolanic materials.

Another important factor influencing the level of C_{crit} is the quality of the steel/concrete interface. It was early recognised that solid hydration products on the steel surface protect the steel, both by acting as physical barrier as well as – particularly in the case of $Ca(OH)_2$ – by buffering the pH in the pore solution at the steel surface [34-35]. There is a general consensus that this is one of the reasons for higher chloride threshold values of steel embedded in concrete as compared with steel immersed in alkaline solutions, e.g. Refs. [56-57]. A detailed review on the effect of the interfacial zone on chloride induced corrosion is given in Ref. [38]. The influence of macroscopic and microscopic defects at the steel/concrete interface has also been discussed in papers VIII and IX.

Chloride binding capacity

In concrete, chloride can be chemically bound in compounds like Friedel's salt, physically adsorbed to the cement paste, and dissolved in the pore solution [58-59]. The latter are usually termed *free chlorides*. There is an equilibrium between bound (chemically and physically) and free chlorides. Main factors that affect the chloride binding capacity are type of cement (particularly the content of calcium and iron-calcium aluminates), pH (carbonated vs. non-carbonated concrete), amount of CSH, and temperature [46-47,58-60].

It is generally assumed that only the chlorides that are freely dissolved in the pore solution interact with the steel and lead to depassivation [61]. The chloride binding capacity of concrete is thus important for protection against chloride induced reinforcement corrosion.

Concrete cover and initiation stage

In reinforced concrete structures, the steel is embedded in concrete with a cover thickness of several centimetres. Thus, any species has to penetrate through this *concrete cover* before it can interact with the reinforcement. Of highest practical importance with respect to steel corrosion are ingress of chloride, moisture, oxygen, and carbon dioxide. Penetration of chloride through the concrete cover can, given a sufficiently high concentration at the reinforcement (critical chloride content), lead to local passive film breakdown and induce pitting corrosion. Reaction of carbon dioxide with calcium hydroxide and water (carbonation) decreases the pH of the pore liquid. As apparent from above, this increases the susceptibility to chloride induced corrosion, and, in an extreme case, might even in the absence of chloride lead to loss of passivity and to uniform corrosion.

According to Tuutti's model [62], the service life of reinforced concrete structures can be divided into an *initiation stage* and a *propagation stage*. The initiation stage describes the

time before corrosion initiation, viz. the period during which chloride ingress takes place until the chloride threshold value is reached or the time until the carbonation front reaches the reinforcement. The propagation stage is the period after depassivation when active corrosion takes place. A schematic representation of Tuutti's model is given in Fig. 1 in paper V. It has in the present thesis been found that for chloride induced corrosion, transition from initiation stage to propagation stage is not a one-step-occurrence as schematically assumed in Tuutti's model, but rather a period of time (papers VI, IX, and X).

The time required for chloride to reach the reinforcement steel depends on exposure conditions (environmental chloride load), cover thickness, and concrete properties. The latter describes primarily permeability and chloride binding capacity. As chloride moves through the concrete pore system, part of it is removed from solution by chemical and physical binding, a phenomenon sometimes referred to as *filter-effect*. Given a high chloride binding capacity, this might substantially slow down the increase of chloride concentration in the pore solution of the internal concrete.

Generally, the penetration of chloride through the cover zone is mathematically described by Fick's second law of diffusion (eq. (10)), well recognising that the actual transport mechanisms are by far more complicated than the pure diffusion mechanism assumed for the model. It was, however, found that the empirical assumption of diffusion allows modelling chloride ingress into concrete with reasonable accuracy even for concrete exposed to wetting and drying (splash zone), e.g. Refs. [63-64]. Thus, many models are based on Fick's second law of diffusion and make use of the so-called "error-function solution", typically expressed in the following form (for 1-dimensional ingress):

$$C(x,t) = C_o + (C_s - C_o)\left(1 - erf\left[\frac{x}{2\sqrt{D_a(t)\cdot t}}\right]\right) \tag{11}$$

Here, $C(x,t)$ is the chloride content at depth x and time t; C_o is the initial, uniformly distributed chloride content in the concrete; C_s is the chloride content at the exposed concrete surface; and D_a is the apparent chloride diffusion coefficient. To take into account the proceeding cement hydration, viz. the continuously changing concrete microstructure, the latter is considered as a time-dependent variable, e.g. Refs. [65-67]. Fitting of field and laboratory data has shown that this time-dependency can be empirically described by the following relationship:

$$D_a(t) = D_o \cdot \left(\frac{t_o}{t}\right)^n \tag{12}$$

Here, D_o is a reference apparent diffusion coefficient at reference age t_o; and n is the age factor, which is a constant depending on concrete (binder, w/b ratio, etc). Please note that D_a is referred to as "diffusion coefficient" only because the variable is part of Fick's second law of diffusion; in this context, it is an empirical parameter rather than a true diffusion coefficient. Although it is well accepted that the diffusivity of concrete changes with time (as long as $\alpha < 1$), the approach described in eq. (12) has been subject to controversial discussions in the literature [66,68]. It must also be noted that the "error-function solution" to Fick's second law of

diffusion is based on the assumption of a constant diffusion coefficient. Thus, eq. (11) is mathematically not a correct solution.

Service life modelling

In service life modelling, such as the fib model code [69] or DuraCrete [70], the end of service life is considered reached when the modelled chloride concentration at the depth of reinforcement, *d*, exceeds the critical chloride content, i.e. when

$$C(x = d, t) > C_{crit}\,. \tag{13}$$

In a full-probabilistic approach, all the variables are described in a statistical manner, viz. by a type of probability distribution and the related parameters (normally mean value and variance). This allows calculating the probability for formula (13) being fulfilled, or in other words, the probability for corrosion initiation as a function of time. By defining an acceptable *target probability*, the service life (number of years) can be derived.

The main difficulty regarding practical applications of this approach is the need for reliable input parameters. In general, data to treat all the variables as continuous stochastic parameters with a reasonable level of confidence is absent. To simplify matters, the model might be used in a deterministic manner, i.e. by characterising all the variables by a single value, often mean values. Although this decreases the number of required parameters, the significance of the model outcome is still questionable. Both for probabilistic and deterministic applications, particularly the input parameters n and C_{crit} have a pronounced influence on the computed service life [66,68]. Being aware of the difficulties associated with service life calculations, it has been proposed to use the models only as a tool to compare various technical solutions at a design stage (e.g. binders and cover depths) rather than trying to predict the service life, see e.g. Ref. [71]. Nevertheless, this does not eliminate the need for reliable input parameters and the large uncertainties inherent to at least some of them might bias the results.

Corrosion conditions and propagation stage

Once stable pitting corrosion has established, the corrosion rate is governed by the kinetics of the reaction steps as discussed in section 3.1, viz. the anodic reaction, the cathodic reaction, and the ionic current flow in the macro-cell. For steel embedded in concrete these reaction steps might be affected by the following mechanisms:

- *Cathodic reaction*: Atmospherically exposed concrete structures usually contain enough water and oxygen for oxygen reduction to proceed. In the case of submerged concrete, on the other hand, oxygen depletion very likely restricts the cathodic reaction to low rates (cathodic diffusion control).
- *Anodic reaction*: In alkaline, chloride free concrete, the reinforcement is passive and the anodic reaction limits the corrosion rate to negligible levels. In the case of pitting corrosion, transport of ionic species to the pit and away from it takes place (section 3.1).

Having in mind the concrete pore structure, it appears reasonable that the microstructure of the concrete (interconnectivity, pore tortuosity) imposes a resistance against mass transport. Under certain conditions, this might result in anodic diffusion control as discussed in more detail in paper X and the references cited therein.

- *Ohmic control*: In an analogous manner, the concrete microstructure is expected to affect ionic current flow between anodic and cathodic sites (Fig. 2) and thus the *IR drop* (Fig. 3b). In addition to microstructure, also the electrical conductivity of the pore solution, the moisture content in the concrete and temperature play a role for the ohmic resistance in the macro-cell. The electrical conductivity of the pore solution depends on chemical composition, mainly on pH and the presence of other ionic species (chloride, alkali metal ions, etc) [72].
  The electrical *concrete resistivity* is a measure of the ohmic resistance of the concrete against current flow. It involves various parameters such as pore structure (interconnectivity, pore tortuosity), pore solution chemistry, as well as moisture content in the concrete, e.g. Ref. [73]. The ohmic resistance in the macro-cell is a function of both (local) concrete resistivity and geometrical configuration. In dry concrete, as an example, the corrosion process might be under ohmic control since the concrete resistivity increases with declining moisture content.

Both for corrosion owing to chloride ingress and carbonation, it is well documented in the literature that the corrosion rate is (empirically) inversely proportional to concrete resistivity [74-85]. This might be owing to pure ohmic as well as anodic control or a combination of these, as discussed in paper X.

The rate of loss of rebar cross section in the propagation stage can thus empirically be correlated to concrete resistivity. Even after corrosion initiation, concrete structures might be serviceable for a long time as long as the propagation rate is on a negligibly low level. It has in paper X been postulated that the early propagation stage is dominated by anodic control, whereas later stages appear to be under cathodic/ohmic control.

4 SUMMARY OF USED METHODS

In the following, the most important experimental techniques used in the present thesis are briefly summarised.

Potential measurement

An electrochemical potential is always measured versus a reference electrode (RE). An electrical connection has to be established to the electrode of interest (e.g. reinforcement steel or an ion selective electrode) that is usually denoted working electrode (WE). The potential difference between working electrode and reference electrode is then measured with help of a voltmeter.

In order not to disturb the electrode under study, the internal impedance of the measurement instrument should be high. In the present work, the input impedance was at least 10 MΩ for measuring potentials of embedded reinforcement; in the case of embedded ion selective electrodes, which are more prone to being affected by the flow of a measurement current, devices with at least 10 GΩ were used. As external reference electrode, usually commercial saturated calomel electrodes (REF451, Radiometer Analytical, France) were used; as reference electrodes embedded in concrete, manganese dioxide electrodes (ERE 20, Force Technology, Denmark) were used.

Measurement of linear polarisation resistance (LPR)

LPR measurements are generally used to determine the instantaneous corrosion rate of an electrode. The technique is based on the observation that within a small potential range around E_{corr}, the *E-I*-relationship is approximately linear [86]. The linear polarisation resistance is defined as the slope of this curve ($R_p = dE/dI$) at E_{corr}. It can experimentally be obtained in a conventional three-electrode configuration (WE, RE, CE) by polarising the working electrode a few millivolts (typically 10 mV) into anodic and cathodic direction and recording the required current. The well-known Stern-Geary equation allows calculation of the corrosion current [86]:

$$I_{corr} = \frac{B}{R_p} = \frac{\beta_a \cdot \beta_c}{2.3\left(\beta_a + \beta_c\right)} \cdot \frac{1}{R_p} \tag{14}$$

Constant B contains the anodic and cathodic Tafel slopes and is, in the case of reinforcement steel in concrete, usually assumed in the range 26 mV (corroding steel) or 52 mV (passive steel) [87].

If R_p is related to metal area, corrosion current density i_{corr} (mA m^{-2}) instead of corrosion current I_{corr} (mA) is obtained. While in laboratory setups, the area of polarised steel is in general known, this is problematic in the case of field measurements where the reinforcement surface area is practically infinite. Moreover, calculation of corrosion rate from R_p is, strictly speaking, only correct for uniform corrosion; for localised corrosion (chloride induced

corrosion), the area of actively corroding metal is normally unknown. In fact, the anodically acting surface area is variable over time. This is only one example of reasons why the accuracy of corrosion rates (current densities) computed on the basis of R_p measurements is in the case of localised corrosion highly questionable.

Another uncertainty concerning LPR measurements is the ohmic drop (*IR* drop) between the electrodes in the three-electrode-setup that arises from the relatively high electrical resistivity of the concrete (and the flow of current). Since RE is situated somewhere in the current field established between CE and WE, the actual potential of WE differs from the one measured versus RE. If this is not taken into account, the measured polarisation resistance contains, in addition to the true R_p, also the ohmic resistance of the electrode configuration. An uncompensated R_p is thus always higher than the true one. The magnitude of this error depends on several parameters. In the case of passive steel, R_p is usually so high that the ohmic resistance can be neglected. For actively corroding steel, on the other hand, where R_p is low, the *IR* drop might constitute a considerable error, particularly in the case of concrete with high electrical resistivity. Several techniques for ohmic drop compensation have been proposed as reviewed e.g. in Ref. [88]. In the present work, the so-called *current interrupt method* was occasionally used as it was a built-in feature of one of the measurement instruments. In this method, the current is during polarisation periodically interrupted for a short time (typically in the range 1/1000–1/10 s). During interruption, the *IR* drop vanishes immediately (as the current, *I*, is zero) and the potential decreases back to the open circuit potential, the latter process being comparatively slow owing to discharging effects of the double layer. Measurement instruments generally attempt to separate the immediate potential drop from the slower decay and use the former for *IR* drop compensation. Separation of these two effects is, however, associated with uncertainties. Another option used in the present thesis to correct for the ohmic drop is to perform uncompensated LPR measurements and subsequently subtract the ohmic resistance from R_p. The procedure to determine the ohmic resistance in these cases (with a separate measurement) is described in detail in paper VI.

More information regarding the application of LPR to reinforced concrete and its uncertainties can be found in Refs. [89-90].

In the present thesis, LPR measurements were performed with different equipment namely an automated system by Protector AS, Norway, and a Princeton Applied Research Parstat 2273 instrument; further experimental details are given in the respective descriptions of the used setups in the appended papers.

Electrochemical impedance spectroscopy (EIS)

EIS is performed by imposing a sinusoidal voltage signal (alternating current (AC)) with an amplitude typically in the range of 10 mV to the working electrode. The frequency is varied over a large range (usually from MHz to μHz) and the current response in the system is measured. From the relation between the imposed voltage signal, the recorded current response and the phase difference, the impedance, *Z*, can be obtained for various frequencies. The measured

impedance as a function of frequency depends on the system's combination of energy dissipaters (ohmic resistors) and energy storage elements (capacitors).

Considering a simple parallel system of a capacitor and a resistor, for instance, at very low frequencies, the capacitor will act as an insulator (once it is charged), and the current is forced through the resistor; thus, the impedance is equal to the resistor. At high frequencies, on the other hand, the capacitor is short-circuited and the impedance vanishes. At intermediate frequencies, both capacitor and resistor carry the AC current. The relative amounts depend on the frequency of the imposed signal.

With help of equivalent circuits, the measurement results can be interpreted. Equivalent circuits for the case of steel embedded in concrete have been proposed in the literature, e.g. Ref. [91], so that charge transfer resistance, double layer capacitance and ohmic resistance can be calculated. This gives information on the corrosion rate or electrical properties of the bulk concrete.

By using complex notation, impedance is split into a real part, $|Z|\cos(\text{phase angle})$, and an imaginary part, $|Z|\sin(\text{phase angle})$. To discuss the variation of impedance with frequency, the data is then often plotted in a *Nyquist plot* (*complex plane plot*), where real and imaginary parts of the impedance are abscissa and ordinate, respectively. For the example of the simple parallel circuit given above, measurements at a wide range of frequencies would result in a semi-circle passing through the origin with a diameter equal to the ohmic resistor.

More detailed descriptions on theory and application of EIS for steel in concrete or to characterise concrete can be found elsewhere [91-94].

In the present thesis, electrochemical impedance spectra were measured with a Princeton Applied Research Parstat 2273 instrument; further experimental details are given in the appended papers VI, IX, and X that involve EIS measurements.

Electrical resistivity of concrete

Several techniques can be used to measure the (instantaneous) electrical resistivity of concrete [73,95]. In general, they are based on imposing a voltage between two (or more) electrodes and measuring the current (or vice versa) and using a cell constant to convert the measured electrical resistance, R (Ω), into electrical resistivity, ρ (Ωm). The cell constant depends primarily on the configuration of the electrodes and can be obtained by calibration measurements in electrolytes of known conductivity (which is the inverse of resistivity), theoretical approaches such as by mathematical solving or by numerical methods (e.g. finite element modelling).

Electrical resistance measurements can be conducted both with direct current (DC) and alternating current (AC), where it is generally recommended to use (sinusoidal) AC signals to avoid polarising effects at the electrodes [95]. The recommended frequencies to find values representative for DC resistivities (for ordinary, unreinforced concretes) are in the range 50 Hz – 10 kHz [95-96]. Typical commercial hand-held instruments operate at 125 Hz or 1 kHz.

Uncertainties for resistivity measurements are those inherent to the cell constant or the fact that the measured bulk value might not be representative for the application (e.g. the local properties in a corrosion macro-cell as addressed in paper X). Temperature is known to strongly affect resistivity – roughly 3–5% per degree Celsius [95] – and must thus be taken into account to avoid erroneous results when measuring at varying temperatures. A final point that merits comment is that for considerations regarding corrosion mechanisms, DC resistivity is the relevant parameter, while for the reasons pointed out above, common measurement methods rely on AC. This has to be taken into account for systems deviating from traditional materials – for instance in the presence of electrically conductive fibres where AC measurements do not necessarily represent DC properties.

In the experiments described in the present thesis, electrical resistivity was usually measured between embedded steel tubes either with a commercial hand-held LPR meter or an automated system provided by Protector AS, Norway, both of them using an AC signal with a frequency of 1 kHz; further details are given in the appended papers.

Pore solution expression and chemical analysis

By applying tri-axial pressure to a sample of cement paste, mortar or concrete, expression of pore solution is possible [46,59,97]. In the present work, a sample of ca. 100 ml in volume was placed in the apparatus and a maximum pressure of 280 MPa was applied for up to one hour. A more detailed description of the used procedure is given in Ref. [59]. In the present experiments, typically a few millilitres of pore liquid were obtained and kept in vials until chemical analysis. Note that the pore solution expression technique is limited for low w/c ratios, coarse aggregates or rather dry specimens since the amount of expressed pore liquid is too little [98]. Possible uncertainties of this method are addressed in papers I and V.

After pore solution expression, the remaining air in the vials, in which the obtained pore liquid was kept, was in the present work replaced with a CO_2 free gas mixture in order to avoid carbonation during storage. Hydroxide ion concentration was analysed by potentiometric titration and chloride by chromatography. In selected samples, also other ions such as potassium, sodium, calcium, aluminium, iron, or sulphate were analysed. These analytical measurements were performed by a private laboratory (preBIO, Namsos, Norway).

Evaporable and nonevaporable water

As water evaporates at temperatures above 100°C, the weight loss of a concrete sample during drying at 105°C is considered as the amount of evaporable water. When related to the concrete porosity, this allows estimating the degree of capillary saturation (DCS). The weight loss between 105 and 1000°C is termed loss on ignition (LOI), which is usually assumed as the non-evaporable water (chemically bound water). Together with knowledge of the amount of chemically bound water at full hydration ($\alpha = 1$), this allows estimating the degree of hydration.

These measurements were performed in paper IV of the present thesis, where more details regarding determination of DCS and α are provided.

Acid-soluble chloride content

The content of acid-soluble chloride per dry concrete (in % by weight) is usually assumed to represent the total chloride content. In general, the methods are based on homogenising a sample of powdered and dried (often at 105°C) concrete – the volume of the sample being assumed to be representative for the concrete – and dissolving it in acid. The concentration of extracted chloride is then measured by various methods such as titration or spectrophotometry.

Although recommendations and national standards exist, e.g. Refs. [99-101], many laboratories use their own procedures. This has in a world-wide round-robin test [102] been found to result in a large uncertainty for total chloride contents reported by different laboratories. Also the results obtained from one procedure performed by one laboratory typically exhibited a rather high scatter. Some selected results of this round-robin test are shown in Table 3 of paper VII, from which it is apparent that for total chloride contents from 0.4 to 2.0% by cement weight, the measurement uncertainty might well be in the range of 10–25% (with the highest uncertainty at low chloride contents) even for constant method and laboratory.

In the present experiments, the analysis of acid-soluble chlorides was performed by SINTEF Building and Infrastructure in Trondheim with an extraction procedure based on mixing 5 g powdered concrete with 50 ml of 6.5% nitric acid (at 80°C), stirring for 30 s and a dissolution time of 1–3 h (at room temperature). Chloride analysis was performed with a photospectrometric method. The reproducibility of this procedure was roughly estimated on the basis of 4 identical samples taken from homogenised concrete powder with 1.5% total chloride by cement weight. Deviations of the maximum and minimum values with respect to the mean value were in the range 15–30%.

Scanning electron microscopy and X-ray microanalysis

Scanning electron microscopes (SEMs) allow studying materials on a nanometer to micrometer scale. Electrons are generated and accelerated in the so-called electron gun. Electron lenses are used to focus the electron beam to a small spot on the sample surface. Typical SEMs can produce an electron beam with a spot size less than 10 nm. The beam interacts with the specimen to a depth of ca. 1 µm. When the beam hits the sample, different signals are generated, of which the two most often used are backscattered electrons and secondary electrons. When electrons enter the sample they interact as negatively charged particles with the electrical fields of the specimen atoms. They might lose all their energy or might be deviated in such a way to leave the sample at some point (backscattered electrons). Secondary electrons are outer shell electrons that are hit by the electron beam and ejected from the atom. General detectors within the SEMs collect both backscattered electrons as well as secondary

electrons. Image formation can be based on various measurements; the most frequent is the three-dimension-like visualisation of the surface topography. Topographic contrast arises because the number of backscattered and secondary electrons depends on the angle between beam and local surface.

Conventional SEM requires samples to be studied under vacuum owing to the disturbing interference between gas molecules and the electron beam in the chamber. This limits the application to samples that do not produce vapour, e.g. metallic samples such as the ISEs studied in the present work in paper I.

The environmental scanning electron microscope (ESEM), on the other hand, allows studying samples in low-vacuum and high relative humidity environments. Thus, concrete or cement paste samples can be investigated without the need to dry them (which affects the pore structure and causes carbonation).

As a result of the electron bombardment, also characteristic X-rays are emitted from the sample. Typical scanning electron microscopes are nowadays equipped with X-ray detectors such as the energy-dispersive spectrometer (EDS). Analysis of the emitted characteristic X-rays can yield both qualitative identification (elements that are present) and quantitative information from a volume of roughly 1 μm in diameter and 0.5–1 μm in depth.

All of these techniques are described in more detail in the literature, e.g. in Ref. [103].

In the present thesis, SEM microscopy and X-ray microanalysis were at NTNU performed with a JEOL JXA-8500F electron probe micro analyser and at ETH Zurich, Switzerland, with a Quanta 200 3D (FIB) environmental scanning electron microscope by FEI equipped with X-ray detectors Genesis 4000 by EDAX.

5 DISCUSSION OF MAIN FINDINGS AND CONCLUSIONS

5.1 Measuring the free chloride ion concentration in concrete

Direct potentiometry in concrete

Ion selective electrodes (ISEs) are electrochemical sensors that, in an ideal case, are sensitive to a specific ion and assume an electrochemical potential as a function of the ion activity of the respective species. The technique that makes use of this in order to determine the chloride ion activity in a solution is referred to as *direct potentiometry*. Paper I summarises the theoretical background regarding silver/silver chloride electrodes as ISEs embedded in concrete and presents experimental results from applying this technique to measure the chloride ion concentration in the concrete pore solution. Performance of ISEs as non-destructive chloride sensors was studied both in alkaline solutions and in mortar. It was shown that also in highly alkaline environments, the used Ag/AgCl electrodes follow Nernst's law with calibration parameters close to theoretical values (Fig. 2 in paper I). Furthermore, considering interference of hydroxide, the detection limit for chloride ions was lower than 10^{-2} mol/l even at pH close to 14. The electrodes were also found to show good long-term stability in the highly alkaline environments. In summary, it was concluded that Ag/AgCl electrodes are in principle suitable to be used as chloride sensors embedded in concrete.

Diffusion potentials as main error source

Nevertheless, on the basis of the experiments described in paper I, the presence of *diffusion potentials* as main error source for the application of direct potentiometry to concrete was recognised. While the sensors themselves perform well, measurement of the correct ISE potential is the critical step. Paper II gives an overview of diffusion potentials and distinguishes the terms *diffusion potential*, *membrane potential*, and *liquid junction potential* (that are sometimes confused in the literature). In short, the term *diffusion potential* describes the potential drop in general that arises owing to differences in ionic mobilities and the presence of concentration gradients. In the absence of membranes (solid, porous boundaries) between two liquids of different chemical composition, diffusion potentials are more specifically referred to as *liquid junction potentials*; for liquids separated by membranes with *permselective properties*, diffusion potentials are called *membrane potentials* (Fig. 1 in paper II). Permselectivity describes the property of a membrane to decelerate specific ions while not affecting others. Cement paste is generally considered to possess permselective properties owing to the small pore diameters through which ionic transport has to occur and the presence of surface charge on the pore walls. More specifically, cations are believed to be decelerated with respect to anions.

In paper II, the case of liquid junction potentials at the interface of an external reference electrode in contact with a concrete surface was discussed. It was shown that keeping the wetting agent, usually a wet sponge, as conductive as possible (high ionic strength) is beneficial

for reducing the liquid junction potential. Diffusion potentials inside the concrete arising from chloride or pH profiles, on the other hand, cannot be affected. In order to reduce these error sources in the measurement, it was suggested to use embedded reference electrodes. If they are located at the same depth as the ISE, concentration gradients in the measurement circuit can be minimised.

A major factor regarding both liquid junction and internal diffusion potentials (membrane potentials) has been identified to be gradients in pH. Diffusion potentials are thus expected to significantly disturb potential measurements when for instance using an external reference electrode on a carbonated concrete surface to measure the potential of a working electrode at a depth unaffected by carbonation. It was in paper II discussed how the mentioned error source affects different potential measurements, viz. that they are usually of minor concern for condition assessment by potential mapping, but might markedly affect the accuracy of direct potentiometry.

The sensitivity of potentiometric measurements was further discussed in paper III. In particular, a numerical model was used to predict membrane potentials inside concrete arising from realistic chloride or pH gradients. To model permselectivity, values for ionic diffusivities through cement paste were taken from the literature. On this theoretical basis, it was concluded that as long as the pH is above 13.5 (and spatially constant), the membrane potentials arising from chloride concentration gradients of up to ca. 1 mol/l are less than 10 mV (Fig. 4 in paper III). In contrast, even small differences in pH between reference electrode and ISE lead to large diffusion potentials that render the results of the ISE measurement useless (Fig. 3 in paper III). This was also experimentally found in paper I, where the exposure solution in the laboratory – first unintentionally, later on purpose – carbonated, which established pH gradients along the measurement path.

Permselective properties of cement paste

Analysis of the experimental data in paper I in comparison with the theoretical model described in paper III lead to the conclusion that the cement paste is indeed likely to possess permselective properties and, moreover, that these get more pronounced with decreasing w/c ratios.

Finally, in paper IV, the permselective behaviour of cement paste was studied in an experimental setup based on embedded ISEs. The setup allowed measurement of diffusion potentials in concrete for the first time in a moisture state below saturation. In contrast, conventional diffusion cell setups only permit studying the saturated state, which, however, is hardly relevant for practice. Local pore solution compositions and diffusion potentials, arising from chloride and pH gradients, were measured and compared with a theoretical model based on coupled Nernst-Planck equations. This allowed estimation of diffusivities of the most abundant ionic species. As the ratios of these values, i.e. the diffusivities with respect to each other, were close to values tabulated for dilute bulk solutions, it was concluded that the studied mortar (w/c = 0.6, self-desiccation) did not have significant permselective properties. Double layer effects were on a theoretical basis discussed with respect to the size of stably water-filled

capillaries for the actual moisture state (Fig. 14 in paper IV). Apparently, even at this moisture state, the water-filled capillaries are still large enough to allow ionic transport through those fractions of pore solution that are unaffected by double layer effects.

It might however be noted that in paper IV, mixed-in chloride was used. It is well-known that chloride affects the cement hydration kinetics and is thus likely to change the microstructure. Controversial findings regarding the effect of mixed-in chloride on porosity and pore size distribution have been reported in the literature: Whereas Hansson et al. [104] found a coarser pore structure and higher total porosity in the presence of mixed-in chloride, Suryavanshi et al. [105] reported a decrease in total pore volume, particularly affecting the amount of coarse pores. Nevertheless, the pore size distribution seems to play a decisive role for transport of ionic charge through concrete. The pore structure formed in the absence of admixed chloride might show better capillary discontinuity and thus lead to more marked permselectivity (as ionic transport would be forced through narrower pores). Indication for this are the results reported in paper I, which implied some permselective action also in the case of w/c = 0.6 (sealed curing during almost 2 months, then exposed to external chlorides).

Main conclusions

Ion selective electrodes (Ag/AgCl) are in principle suitable for non-destructive determination of chloride ion concentrations in concrete. Correct measurement of the sensor potential is the critical step, particularly in concrete, owing to the likely presence of diffusion potentials. The accuracy is especially adversely affected when pH gradients and chloride profiles arise along the measurement path. The location of the reference electrode with respect to the ISE is thus crucial. As long as the pH is high (above 13.5) and the chloride concentration gradient along the measurement path is below 1 mol/l, small diffusion potentials are established and the accuracy of the free chloride measurement can be expected to be better than ±30% chloride concentration. The uncertainty of the method is thus comparable to the one inherent to common procedures for determination of acid-soluble chlorides (compare section 4 and Ref. [102]). For smaller chloride concentration gradients than the considered, somewhat extreme case of 1 mol/l, the accuracy of the measured free chloride concentration gets better; generally, for lower pH in the pore solution (e.g. in the presence of pozzolanas), however, the accuracy will be negatively affected.

A final comment is to be made on diffusion potentials: Although identified to be a serious error source for direct potentiometry, diffusion potentials can also be considered as source of information since measurement of diffusion (membrane) potentials in concrete provides insight into mechanisms of ionic mass transport through the pore system.

5.2 Concept of critical chloride content

Literature review on critical chloride content

Paper V reviews the concept of critical chloride content (definitions), discusses influencing factors and assesses the techniques commonly used to measure C_{crit}. More than 50 references directly reporting critical chloride contents were evaluated and experimental details collated. Firstly, it was striking that chloride threshold values in the literature scatter over several orders of magnitude, regardless of whether they are expressed in terms of total chloride (per cement/concrete weight) or free chloride (per cement/concrete weight, in mol/l in the pore solution) (Figs. 2 and 3 in paper V). This scatter could at least partly be explained by the large variety of used experimental setups. Moreover, it appeared that certain parameters inherent to the test procedure can have more dominant influences on the measured C_{crit} than the parameters under investigation. For instance, polarising the rebar to a fixed potential (potentiostatic control) rather than leaving it assume the corrosion potential freely, generally resulted in lower threshold values. This is in agreement with the results of experiments studying free and polarised rebars as reported elsewhere [106].

It was also concluded in paper V that many of the reported chloride threshold values are not practice-related owing to unrealistic experimental setups. For instance, many authors used smooth instead of ribbed steel, and the surface was only in a minority of cases in as-received condition; chloride was often introduced in the fresh mix (Fig. 7 in paper V). Moreover, critical chloride contents for cement types other than CEM I were contradictory. On this basis, from an engineering viewpoint, the current practice of condition assessment or service life predictions cannot be improved. Generally, consultant engineers base their decisions on long-term experience from existing structures (mostly Portland cement) and use threshold values in the range of 0.4–0.6% chloride by binder weight. However, it appears questionable what reasons other than the absence of better knowledge would justify the common practice of applying these threshold values also to modern binders that contain significant proportions of non-Portland cement components.

To be able to assess the effect of non-traditional binders on the corrosion performance, for instance regarding C_{crit} as input parameter for service life models, it was in paper V concluded that there is a strong need for a practice-related test method for C_{crit}. Specific recommendations for experimental parameters were made; it was suggested to use *ribbed* steel bars in *as-received* condition, chloride introduction by *capillary suction* and/or *diffusion* (wetting/drying cycles), and to leave the steel at its *free corrosion potential*. Experimental support for the latter recommendation was also obtained in paper VI as discussed in section 5.3.

Size effect of critical chloride content

The concept of critical chloride content was further discussed in paper VII. From literature data regarding pitting potentials measured in aqueous solutions, it is apparent that the size of the studied specimen is decisive for its corrosion performance (Fig. 1 in paper VII). This was ascribed to the localised nature of pitting corrosion and the probability for likely initiation sites

within a given metal area. The concept was in paper VII applied to concrete by considering both the stochastic character of metallurgic irregularities as well as the variable properties of the ITZ. A probabilistic model was used to describe the effect of specimen size on the statistical distribution of C_{crit}. Based on literature data for the probability distribution of corrosion initiation as a function of chloride content in the concrete, the distribution of C_{crit} was predicted for increasing specimen size (Figs. 4 and 5 in paper VII). It was shown that both the variance as well as the mean value decrease with increasing rebar length (exposed metal area). Please note that in the literature, data describing the statistical distribution of C_{crit} (for a certain specimen size) is scarce. Only two references were in this regard found to be useful, the one by Breit [107] and the one by Zimmermann [108]. As a matter of course, the reliability of this data is limited in many regards. For instance, it is open to question if the number of values acquired in Refs. [107-108] is sufficient to describe the statistical distribution of C_{crit} with a reasonable level of confidence. Experimental parameters such as potentiostatic control in Ref. [107] versus free corrosion potential in Ref. [108], surface condition of the steel, sampling procedures for chloride analysis, rebar orientation during casting and direction of chloride ingress, or concrete mix details might have lead to unrealistic results. The limitations inherent to the data used as a basis for application of the probabilistic model in paper VII have to be born in mind. The results of combining the probabilistic model with the data from Refs. [107-108] have thus only illustrative character.

The implications of the size effect were in paper VII discussed with regard to test methods and service life modelling. Considering test methods, the lower variance for increasing specimen size implied that less parallel specimens are required when using larger specimens in order to achieve the same level of confidence for the measured values (Fig. 6 in paper VII). Given the variances obtained from the probabilistic model of paper VII and the data from Refs. [107-108] it was, however, concluded that the expected accuracy of practical test methods (practical with respect to number of parallel specimens and their size) might be rather poor.

Critical chloride content as input parameter for service life models

The fact that C_{crit} appears to depend on the size of the specimen on which it is measured raised fundamental questions regarding the concept of critical chloride content and service life modelling. How to deal with the obvious discrepancy between laboratory samples of a few decimetres in length and realistic structures that are several thousand times larger? Is it correct to use C_{crit}, measured on relatively small laboratory specimens, for service life models of real-life-size reinforced concrete structures?

Considering that the measurement of the critical chloride content essentially is a minimum value problem, viz. the weakest point in a specimen is ascribed with the chloride content C_{crit}, the probability for corrosion initiation must indeed be linked to the rebar length. From this it was in paper VII inferred that, strictly speaking, the critical chloride content measured on specimens of a certain size can only be used to predict the service life of identical specimens, and not for larger (or smaller) ones. This lead to the suggestion of taking into account the static behaviour of the structural member under study in order to derive the length that is relevant from structural viewpoints (Fig. 7 in paper VII). It was proposed to term this length

characteristic structural length, which was defined as the length, l, within which initiation of one pit is critical regardless of the location of corrosion-onset. Consider as an example a static system as the one depicted in Fig. 6a, where the load-bearing capacity is equally compromised for the three different cases of local corrosion onset within l indicated by A, B, and C.

It was suggested that this characteristic length is the length relevant for C_{crit} to be used in modelling the probability for corrosion initiation and predicting the service life. The input parameter C_{crit} should thus either be measured on specimens of the relevant characteristic length, or, when measured on smaller samples, the probabilistic model in paper VII could be used to transform the variable to be valid for this length.

Finally, these considerations enabled a better understanding of the term "probability of corrosion initiation". In a probabilistic service life calculation, this probability is compared with the so-called target probability, p_{target}. However, there is no consensus among researchers or practical engineers regarding the meaning of this corrosion probability and values for the acceptable target probability are commonly selected on a questionable basis. It was in paper VII suggested how the acceptable failure probability for probabilistic service life modelling could be selected on the basis of structural considerations. In the example shown in Fig. 6, the variable F describes the tensile forces in a cross section located within the characteristic length (F can be obtained from static calculations). As rebars are supplied in fixed standard diameters and civil engineers usually select practical values for the rebar spacing, the tensile capacity, R, is always higher than F. Let the utilisation ratio, F/R, in the present example be 90%. This means that it is tolerable that 1 out of 10 steel bars of the lower reinforcement in the cross section depicted in Fig. 6b corrodes through. As a conservative simplification the propagation stage might be neglected, viz. the service life might be considered reached as soon as 1 out of 10 rebars initiates corrosion. Thus, for a probabilistic service life calculation of the cross section shown in Fig. 6b, the tolerable probability of reinforcement corrosion within the characteristic length becomes 10% (target probability). This in turn means that when performing experiments with specimens of the same length, l, the chloride content relevant for the service life model (C_{crit}), is the one at which 10% of the experimental test specimens depassivate. When using smaller (or larger) specimens in the test setup, this percentage is shifted according to the probabilistic model presented in paper VII.

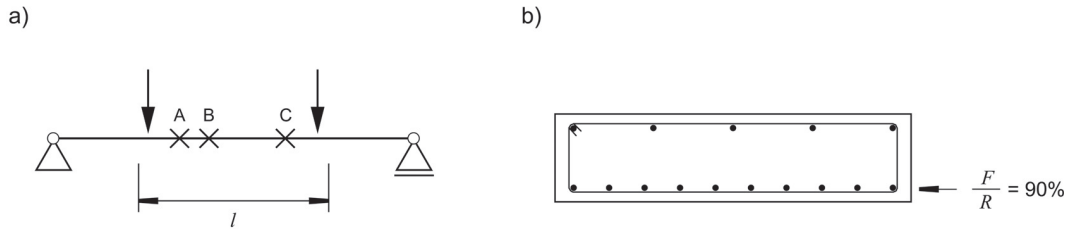

Fig. 6. Static system (a) with characteristic structural length, l, where the bending moment and thus the tensile force, F, in the lower reinforcemet in the cross section (b) are constant. A, B, C = schematic illustration of possible locations of corrosion onset; R = tensile capacity of lower reinforcement in the cross section.

Of course, the simplification of neglecting the propagation stage, made above, does not describe reality properly. If the probability of corrosion is to be related to tolerable loss of steel cross section (and thus load bearing capacity), the propagation stage has to be taken into account since at the time of depassivation, no significant loss of cross section has yet occurred. As an extreme example, one might consider that half of the rebars depassivate (50% corrosion probability), but since the corrosion rate is very low, almost no cross section is lost during decades of years; in another extreme case, only 1 out of 20 rebars might depassivate (5% corrosion probability), but if the corrosion rate is high and this rebar corrodes through within a few years, the loss of cross section might be higher than in the first example. However, current knowledge is not sufficient to allow prediction of corrosion propagation in a reliable manner in order to take cross section loss after depassivation into account and thereby provide holistic probabilistic service life models.

5.3 Mechanism of chloride induced corrosion

Experimental observations regarding C_{crit}

In papers VI and VIII–X, based on the conclusions of paper V, an experimental setup was selected in order to study the corrosion performance of various concrete mixes. In short, ribbed rebars were used in as-received condition, chloride was introduced by wetting/drying cycles (capillary suction and diffusion), and the steel of interest was not polarised (apart from temporary LPR and EIS measurements). In addition, ion selective electrodes were embedded at depth 10 mm, viz. at the cover depth of the working electrode (rebar), and used to non-destructively and thus continuously monitor the free chloride ion activity in the pore solution as described in paper I. The ISE potentials were measured versus an embedded reference electrode located in the same plane (and thus at the same depth as the ISEs with respect to chloride ingress). As no significant pH and chloride concentration gradients were expected to be present in this plane, the effect of diffusion potential errors (papers I–IV) was considered small and the measurements reliable.

During exposure to chloride by wetting and drying, a variety of parameters was continuously monitored by an automatic data logging system several times per day (papers VI, IX, and X) or periodically measured manually (paper VIII). The most important findings regarding critical chloride content were the following:

- The effect of the steel/concrete interface on chloride induced corrosion: i) the rebar orientation during casting strongly affects the location of corrosion onset as for horizontal rebars, corrosion initiated preferentially on the lower rebar side no matter the direction of chloride ingress; ii) the location of corrosion never coincided with macro pores or air voids (papers VI, VIII, and IX).
- Under the present conditions (free corrosion potential, wetting/drying cycles, etc) transition from passive to stable active corrosion can occur over a long period of time. After the first depassivation event, repassivation took often place and further increase of chloride content at the rebar surface was required to enable stable pit growth (papers VI, VIII, and IX).
- The chloride contents required to initiate corrosion were comparatively high; in addition, the values scattered over a wide range (papers VI, VIII, and IX).

Steel concrete interface

The fact that corrosion preferentially initiated on the lower rebar side was ascribed to different properties of the steel/concrete interface formed on the upper and lower sides of the reinforcement during casting and hardening. Investigations by means of scanning electron microscopy, summarised in paper IX, have shown that the microstructure is indeed different on these two sides. A bleed-water zone of 100–200 μm in width has been observed at the underside of the rebar in various specimens of different concrete mixes (Fig. 7 in paper IX). Mainly plastic settlement and collection of bleeding water underneath the rebar are believed to be the reasons for the formation of this zone.

It was in papers VIII and IX suggested that the main parameter determining the local susceptibility to corrosion at interfacial defects is the moisture state. This in turn depends on the exposure conditions. While large pores such as air voids or gaps of several hundreds of micrometres in size would be saturated under submerged conditions (at least on the long-term), they clearly do not fill up in the case of wetting/drying cycles owing to the absence of capillary forces. Thus, in the experiments of the present thesis, macro pores at the steel/concrete interface are considered harmless defects since they are essentially air-filled. This agrees well with the observation that corrosion never coincided with the location of air voids (papers VI, VIII, and IX).

The backscattered electron micrographs presented in paper IX reveal that the bleed-water zone consisted in the present work of large gaps (100–200 µm in width) interspersed with porous zones of crumbly appearance. The latter are composed of a loose conglomerate of cement hydration products as well as aggregate particles with interspaces and pores covering a range of sizes down to diameters that reasonably can be assumed to be stably water-filled at internal relative humidities below 100%. It was suggested that these parts of the bleed-water zone are likely to offer paths for almost unhindered chloride transport to the steel surface. This would both increase the risk of depassivation as well as ensure chloride supply to sustain pitting after depassivation (and make repassivation unlikely).

As an implication of the effect of casting direction, it was in paper IX discussed that the rebar orientation is decisive for a test method for C_{crit}. Apparently, the critical chloride content is different on upper and lower sides of the rebar (for horizontal orientation during casting), and thus, the direction of chloride ingress with respect to casting direction is relevant. This has to be considered when designing or making recommendations for a test method for chloride threshold values.

Corrosion-onset

Thanks to the high time-resolution of the data logging equipment, depassivation/repassivation events were observed in the present thesis. This is not surprising, as in corrosion science, it is well known that many nucleated pits never achieve stable growth. The findings in papers VI and VIII–X have, however, implications for test methods aimed at measuring practice-related C_{crit}. In paper VI, it was suggested that the chloride content associated with stable pit growth is more relevant than the one determined at the very first signs of depassivation. If service life models are to be applied to practical conditions, the latter will be too conservative.

Although not experimentally tested, it can be assumed that potentiostatic control would lead to stable pit growth earlier than under open circuit conditions since the potentiostat heavily sustains the corrosion process (once initiated). An observation supporting this is the fact that under potentiostatic polarisation, clearly visible pits were found in Ref. [109] within hours after depassivation detection, while in the present work (papers VI and VIII–X) after reaching stable corrosion, days or even weeks were required to produce pits of similar size. As potentiostatic control results in C_{crit} being measured at the first depassivation event, it can be expected to yield lower chloride threshold values than a method that takes stable pit growth (after possible repassivation events) as criterion to determine C_{crit}. This is in agreement with Ref. [106] and the literature review in paper V.

Scatter and high level of observed C_{crit}

The observation that the chloride threshold values found in the present thesis varied markedly (papers VI, VIII, and IX) may be explained by the stochastic nature of pitting initiation. Also the level of the observed C_{crit} was generally rather high. When ignoring binder type and w/b ratio, the values were roughly 0.8–3.1% chloride by binder weight (in one extreme case ~3.6%) for upper and vertical sides of the rebar and ~0–1.5% chloride by binder weight (in two extreme cases ~2.9%) for the lower side of the rebar (where the bleed-water zone had formed) (papers VI and IX). Note that in some cases, these values are even minimum values since no corrosion initiated. When compared with the literature (paper V), these C_{crit} appear generally high, although also other researchers have from laboratory studies reported chloride threshold values exceeding 1% chloride by binder weight and up to 3.1% chloride by binder weight [57,84,108,110-116].

A common explanation for the rather high threshold values found in the laboratory as compared to site concrete is the higher quality of laboratory concrete compared with realistic field concrete (more controlled compaction, etc). Considering the observed large air voids entrapped at the steel surface and the bleed-water zone formed on the rebar underside (papers VI, VIII, and IX) the concrete of the present experiments is far from defect-free. However, it might be possible that while in the present study, generally the side on top of the rebar during casting was exposed to chloride, this was not the case in many of the references reviewed in paper V. This hypothesis can, however, unfortunately not be checked since many authors did not describe the test setup in a manner detailed enough to indicate the orientation of the reinforcement during casting.

An alternative explanation for both the high level of threshold values and the large scatter would be the specimen size as discussed in paper VII. Unfortunately, the considerations regarding specimen size (paper VII) were not yet made at the time of planning the experimental setup used in papers VI and VIII–X. From today's standpoint, it would have been better to design larger specimens. When checking the specimen size in the references reviewed in paper V, it is apparent that many researchers used rebar lengths in the range 5–30 cm. From the data, no relation between specimen size and C_{crit} is however, apparent, as this is overshadowed by other experimental parameters.

Experimental observations regarding early pitting corrosion

Finally, once corrosion had started, the process of early pitting corrosion in concrete was studied by monitoring the corrosion potential and polarisation resistance as well as by frequently (almost on a daily basis) measuring the galvanic current that flows when additional cathodic area is connected to the corroding rebar (paper X). The geometrical configuration was such that this short-circuiting with additional passive metal area could more be considered as reducing the ohmic resistance in the system than a simple increase in cathode area. In the very beginning, this enhanced the corrosion rate somewhat, but as pit growth proceeded, the extent to which short-circuiting increased the corrosion rate diminished markedly. It was concluded that the corrosion rate is initially dominated by mixed ohmic and anodic control, but as the

anodic reaction kinetics get more restricted with time, the process gets almost entirely under anodic control. This could be satisfactorily explained by the conceptual model of the microstructure of the cement paste being responsible for limiting mass transport from and to the anode (pit) so that the anodic reaction step gets under diffusion control. Indication for this was, amongst others, the observation that the concrete resistivity correlated well with the extent to which the anodic reaction rate became limited (maximum achieved corrosion rate).

An implication of this is that for a laboratory method to measure chloride threshold values, the specimen size is from an electrochemical viewpoint not critical. Once the conditions for pit nucleation are fulfilled somewhere on the rebar under study, the cathode will not be the limiting factor in deciding whether the pit will survive the metastable phase and achieve stable growth or not. It might in this context, however, be mentioned that paper VII illustrated the importance of specimen size from other viewpoints.

5.4 Main conclusions regarding critical chloride content and mechanism of chloride induced corrosion

It is well known that in a material such as concrete, many parameters exhibit significant statistical variability. This was also apparent in the present thesis, both regarding the local chloride ion concentration in the concrete pore solution (papers VI and IX) and the critical chloride content (papers VI, VIII, and IX). If, in order to estimate the risk of corrosion, the chloride content in the concrete is to be compared with C_{crit}, large uncertainties arise thus from the scatter of the variables. The only way to deal with this in a reasonable manner is the use of probabilistic approaches that treat all the parameters as stochastic variables. This was recognised by the research community and lead to the development of probabilistic service life models. However, if these models are to provide output – such as a predicted service life or a required cover depth for a given time of serviceability – with a reasonable level of confidence, reliable input parameters are required. The literature review in paper V has shown that the published data on C_{crit} does at present not offer a basis to improve service life predictions. The reported values for C_{crit} are not consistent, particularly with respect to non-traditional cement types. This was explained by the fact that experimental parameters of test setups are in some cases likely to have a more pronounced effect on the measurement results than the parameters under study (cement type, w/b ratio, etc). Moreover, little is known about the stochastic variance of C_{crit}. This lack of knowledge is due to insufficient numbers of parallel specimens tested or questionable data reporting such as for instance only mean values.

The only way to improve the state of the art is to reach agreement on a test method for C_{crit} that is suitable to provide practice-related results and information on the stochastic distribution of the variable. In this regard, based on the literature evaluation (paper V), recommendations for certain experimental parameters were made (ribbed steel, as-received condition, chloride exposure by wetting/drying, free corrosion potential). Experimental observations regarding the depassivation behaviour of steel under non-polarised conditions further lead to the suggestion that for practice, the chloride content associated with stable pit growth is relevant rather than the one determined at the very first signs of depassivation (paper VI).

In common experimental setups to determine C_{crit}, specimens with rebars of 5–30 cm in length are used although there is no evidence that these are large enough to reveal results relevant for practice (paper VII). While it was concluded that even in rather small laboratory specimens, the cathode is sufficiently large to provide realistic conditions for (early) pitting corrosion (paper X), probabilistic considerations have illustrated that the specimen size is likely to significantly influence the measured critical chloride content (paper VII). More specifically, the smaller the specimens are (exposed metal area), the higher is the expected mean value of C_{crit} and the wider scatter the measured values. It was in paper VII further discussed how the size effect influences the concept of critical chloride content and service life modelling in general. It was suggested that structural behaviour, i.e. the static system, has to be taken into account for service life calculations in order to consider the specimen size effect (characteristic length).

Regarding corrosion performance, the steel/concrete interface was found to be the most important influencing factor (papers VI, VIII, and IX). Corrosion initiated preferentially on the lower rebar side with respect to casting direction no matter the direction of chloride ingress. Investigations by means of scanning electron microscopy revealed microstructural differences

of top and lower sides, in particular the presence of a bleed-water zone below the reinforcement (paper IX). Formation of this was explained by plastic settlement and bleeding underneath the reinforcement. A main implication of this concerns test setups for C_{crit}: Rebar orientation during casting and direction of chloride ingress into the specimens are decisive for the level of obtained chloride threshold values.

Measurements after depassivation provided insight into the mechanism of early pitting corrosion and lead to the conclusion that the corrosion kinetics are at this stage dominated by anodic diffusion control (paper X). Other investigations reported in the literature focused on later phases in the propagation stage, generally with setups using artificial macro-cells with heavily corroding and large anodes. They concluded that at this stage, the corrosion rate is under ohmic/cathodic control. Regarding models for the propagation stage, it is at present unknown if both the type of corrosion control during early and late stage pitting corrosion as well as the transition between these two are relevant.

6 FURTHER RESEARCH WORK

On the basis of the work undertaken in the present thesis, the following recommendations for future research are given:

Chloride sensors in concrete

It was shown that diffusion potentials between reference electrode and ion selective electrodes (ISE) might significantly disturb the accuracy of this non-destructive measurement technique for the free chloride ion activity in the concrete pore solution (papers I–III). Further research should aim at optimising the measurement system by e.g. developing combined sensors that include both an ISE and a reference electrode. Such a sensor should preferentially not be too large in size and, if to be applied in practice, allow production at reasonable costs.

Permselective properties of cement paste

The setup used in paper IV has proven to be suitable to study diffusion potentials and permselectivity at a moisture state below saturation. On a theoretical basis, it is expected that the effect of permselectivity increases with decreasing w/c ratio and/or decreasing degree of capillary saturation (internal moisture state). This has, however, yet to be validated by further experimental work. Limitations to this might be the fact that studying the liquid phase by pore solution expression becomes difficult when reducing the w/c ratio and the moisture content. Attempts should be made at w/c ratios where capillary discontinuity is achieved and permselectivity can be expected to be more pronounced (probably even at saturation).

Size effect on chloride threshold values

Although there is no reason to believe that the size effect for the susceptibility to pitting corrosion observed for metals in aqueous solutions is not valid for the case of steel embedded in concrete, this has yet to be confirmed experimentally. An experimental study involving a high number of parallel samples would in addition yield detailed information on the statistic distribution of the variable C_{crit} (for a certain specimen size), viz. mean value, variance, and the type of distribution. This is considered crucial for probabilistic service life modelling (paper VII).

Probabilistic service life modelling

Once experimental knowledge on the statistic distribution of C_{crit} for various specimen sizes is known, probabilistic service life modelling might be improved significantly. In paper VII, it has

briefly been outlined how structural considerations on static behaviour could be taken as a basis for selecting the failure probability used in probabilistic models. Such considerations, e.g. the proposed *characteristic length*, would also serve as a basis for selecting appropriate C_{crit} (by taking into account specimen size). Nevertheless, the concept must be improved further. For instance, it was in paper VII not discussed on what basis the characteristic length should be derived, viz. if the utilisation ratio of tensile forces and tensile strength is to be considered on a serviceability or design level (partial safety factors). Furthermore, if the probability of corrosion is to be related to tolerable loss of steel cross section (and thus load bearing capacity), the propagation stage has to be taken into account. In addition, it would be interesting to investigate if the statistic variable C_{crit} when determined with a practice-related laboratory setup and translated into terms of typical characteristic lengths results in computed service lives that one would term "realistic" (e.g. case studies of existing structures).

Role of bleed-water zone for corrosion initiation

In the present study, formation of a bleed-water zone on the underside of the reinforcement steel was found for rebars horizontally orientated during casting (paper IX). This zone at the steel/concrete interface is believed to play a major role for corrosion initiation, viz. to present areas particularly susceptible to chloride induced corrosion. The zone was also found to form when using fly ash and comparatively high slumps in the range of 200 mm. Further research has to study if these interfacial defects can be reduced by means of concrete technology (binder types, workability, ev. self compacting concrete) to an extent sufficient to increase the resistance against chloride induced corrosion.

Propagation stage of pitting corrosion

While the present study has shown that early pitting corrosion of reinforcement in concrete is primarily under anodic control, other investigations focussing on later stages in the propagation phase – often by using artificial macro-cells with heavily corroding and large anodes – have concluded that the corrosion process is under ohmic and/or cathodic control (compare paper X and the references cited therein). Apparently, at some point, the type of corrosion control shifts from anodic to cathodic or ohmic control. It is at present unknown when this transition occurs. Although current service life models generally only consider the initiation phase, attempts have been and are made to model also the propagation phase. It would be valuable to clarify to what extent corrosion has to propagate until cathodic and ohmic control become rate limiting. Knowledge of the transition will be decisive to assess if both the initial corrosion mechanism (anodic control) and the late stage mechanism (cathodic/ohmic control) are relevant for modelling the propagation stage.

Test method for the critical chloride content

The present study has repeatedly indicated that various experimental parameters can substantially affect the level of C_{crit} obtained from a test setup. In this regard, it is recommended that further research and discussion (e.g. in RILEM technical committee CTC [14]) has to focus on the following points:

- What laboratory casting and compaction procedure leads to a realistic steel/concrete interface? Which side of the reinforcement (bleed-water zone or upper side) should be exposed to chloride ingress?
- What is an optimum compromise between specimen size and number of parallel specimens in order to achieve a reasonable level of confidence of the measurement results? How many parallel specimens are needed to describe the stochastic variable sufficiently accurate for the purpose of probabilistic service life modelling?
- What is the relevant point in time for measuring the chloride content with respect to depassivation? The effect of various electrochemical techniques (e.g. potentiostatic control versus free corrosion potential) on corrosion onset should be investigated in more detail.

7 REFERENCES

1. Annual Bridge Inventory 2010, Better Roads Nov (2010), available from www.betterroads.com.
2. M. Yunovich, N.G. Thompson, T. Balvanyos, L. Lave, Corrosion cost and preventive strategies in the united states - appendix D: highway bridges, available from www.corrosioncost.com, Office of Infrastructure Research and Development, Federal Highway Administration, 2001.
3. The World Factbook, Central Intelligence Agency, Washington, DC, available from www.cia.gov/library/publications/the-world-factbook, 2009.
4. Die Aufgaben des ASTRA, Swiss Federal Roads Office / Bundesamt für Strassen ASTRA, available at www.astra.admin.ch, 2009. (in German)
5. H. Ungricht, F. Hunkeler, Massnahmen gegen chloridinduzierte Korrosion und zur Erhöhung der Dauerhaftigkeit, VSS Forschungsbericht Heft 628, Schweizerische Eidgenossenschaft, Bundesamt für Strassen, 2008. (in German)
6. Web page: US Department of Transportation, Federal Highway Administration, http://ops.fhwa.dot.gov/weather/weather_events/snow_ice.htm.
7. Highway deicing - comparing salt and calcium magnesium acetate, special report 235, Transportation Research Board, National Research Council, Washington, DC, 1991.
8. European Standard EN 197-1 "Cement - part 1: Composition, specifications and conformity criteria for common cements", 2000, European Committee for Standardization.
9. European Standard EN 206-1 "Concrete - Part 1: Specification, performance, production and conformity", 2000, European Committee for Standardization.
10. K. de Weerdt, Blended cement with reduced CO_2 emission - utilizing the fly ash-limestone synergy, PhD Thesis, SINTEF Building and Infrastructure / NTNU Department of Structural Engineering, Trondheim, Norway, 2011.
11. K. Van Breugel, G. Ye, Y. Yuan (Eds.), Proc. 2nd Int. Symp. on Service Life Design for Infrastructure, 4-6 October 2010, Delft, The Netherlands, Vol. 1 and 2, 2010, Rilem Publications S.A.R.L.
12. NT Build 355: Concrete, mortar and cement based repair materials: chloride diffusion coefficient from migration cell experiments, 1997, Nordtest, Espoo, Finland.
13. NT Build 443: Concrete, hardened: accelerated chloride penetration, 1995, Nordtest, Espoo, Finland.
14. RILEM technical committee CTC "Corrosion initiating chloride threshold concentrations in concrete", www.rilem.net, activity started in 2009.
15. M. Durand-Charre, Microstructure of Steels and Cast Irons, Springer, Berlin, 2003.
16. M. Pourbaix, Lectures on electrochemical corrosion, Plenum Press, New York/London, 1973.
17. M. Pourbaix, Atlas d'équilibres électrochimiques, Centre Belge d'Etude de la Corrosion CEBELCOR / Gauthier-Villars & Cie, Paris, 1963.
18. A. Pourbaix, Localized corrosion: behaviour and protection mechanisms, in: A. Turnbull (Ed.), Corrosion Chemistry within Pits, Crevices and Cracks, Teddington, Middlesex, National Physical Laboratory, 1984, pp. 1-15.
19. L.L. Shreir, R.A. Jarman, G.T. Burstein (Eds.), Corrosion, 3rd Ed., Vol. 1, 1994, Butterworth Heinemann, Oxford.
20. H.-H. Strehblow, Mechanisms of Pitting Corrosion, in: P. Marcus (Ed.) Corrosion Mechanisms in Theory and Practice, 2nd ed., Marcel Dekker Inc., New York, 2002, pp. 243-285.
21. G.T. Burstein, P.C. Pistorius, S.P. Mattin, The nucleation and growth of corrosion pits on stainless steel, Corros. Sci. 35 (1993) 57-62.
22. H.W. Pickering, R.P. Frankenthal, On the mechanism of localised corrosion of iron and stainless steel, J. Electrochem. Soc. 119 (1972) 1297-1304.
23. J. Bensted, P. Barnes (Eds.), Structure and Performance of Cements, 2nd Ed., 2002, Spon Press, London.
24. T.C. Powers, T.L. Brownyard, Studies of the Physical Properties of Hardened Portland Cement Paste, Bulletin 22, Research Laboratories of the Portland Cement Association, 1948.
25. T.C. Powers, L.E. Copeland, H.M. Mann, Capillary continuity or discontinuity in cement pastes, J. PCA Res. Dev. Lab. May (1959) 38-48.

26. M.R. Nokken, R.D. Hooton, Discontinuous Capillary Porosity in Concrete – Does it Exist?, in: J. Weiss, K. Kovler, J. Marchand, S. Mindess (Eds.), Int. Symp. on Advances in Concrete through Science and Engineering, Evanston, Illinois, Rilem, 2004.
27. G. Ye, Percolation of capillary pores in hardening cement pastes, Cem. Concr. Res. 35 (2005) 167-176.
28. S. Diamond, Physical and chemical characteristics of cement composites, in: C.L. Page, M.M. Page (Eds.), Durability of concrete and cement composites, Woodhead Publishing Ltd., Cambridge, 2007, pp. 10-44.
29. A.M. Neville, Properties of Concrete, 4th ed, Longman Ltd, 1995.
30. P. Grübl, H. Weigler, S. Karl, Beton, 2nd ed, Ernst & Sohn, Berlin, 2001. (in German)
31. L. Bertolini, B. Elsener, P. Pedeferri, R. Polder, Corrosion of steel in concrete, WILEY VCH, Weinheim, 2004.
32. T.C. Powers, Physical Properties of Cement Paste, Proc. 4th Int. Symp. Chemistry of Cement, Washington, D.C., 1960, pp. 577-613.
33. J.C. Maso (Ed.) Interfacial Transition Zone in Concrete, 1996, E & FN Spon, London.
34. A. Bäumel, Die Auswirkung von Betonzusatzmitteln auf das Korrosionsverhalten von Stahl in Beton, Zement-Kalk-Gips 7 (1959) 294-305. (in German)
35. C.L. Page, Mechanism of corrosion protection in reinforced concrete marine structures, Nature 258 (1975) 514-515.
36. M.N. Al Khalaf, C.L. Page, Steel/mortar interfaces: Microstructural features and mode of failure, Cem. Concr. Res. 9 (1979) 197-207.
37. A.T. Horne, I.G. Richardson, R.M.D. Brydson, Quantitative analysis of the microstructure of interfaces in steel reinforced concrete, Cem. Concr. Res. 37 (2007) 1613-1623.
38. C.L. Page, Initiation of chloride-induced corrosion of steel in concrete: role of the interfacial zone, Mater. Corros. 60 (2009) 586-592.
39. L.-O. Nilsson, Hygroscopic moisture in concrete - drying, measurements & related material properties, Report TVBM-1003, Division of Building Materials, Lund Institute of Technology, 1980.
40. S. Rostam, R.F.M. Bakker, A.W. Beeby, G. Hartl, D.v. Nieuwenburg, P. Schiessl, L. Sentler, A.P.v. Vugt, Durable Concrete Structures, 2nd ed, Comité Euro-International du Béton, Lausanne, Switzerland / Thomas Telford Services Ltd., 1989.
41. R.H. Relling, E.J. Sellevold, In situ moisture state of coastal concrete bridges, in: M.G. Alexander, H.-D. Beushausen, F. Dehn, P. Moyo (Eds.), Proc. Int. Conf. on Concrete Repair, Rehabilitation and Retrofitting, Cape Town, South Africa, Taylor & Francis/Balkema, The Netherlands, 2006, pp. p. 191.
42. T.C. Powers, Structure and physical properties of hardened Portland cement paste, J. Am. Ceram. Soc. 41 (1958) 1-6.
43. T.C. Powers, L.E. Copeland, J.C. Hayes, H.M. Mann, Permeability of Portland Cement Paste, J. Amer. Concr. Ins. 51 (1954) 285-298.
44. J.O.M. Bockris, A.K.N. Reddy, Modern electrochemistry, Vol. 1: Ionics, 2nd ed, Plenum Press, New York, 2000.
45. K. Byfors, Influence of silica fume and flyash on chloride diffusion and pH values in cement paste, Cem. Concr. Res. 17 (1987) 115-130.
46. J. Tritthart, Chloride binding in cement. I. Investigations to determine the composition of porewater in hardened cement, Cem. Concr. Res. 19 (1989) 586-594.
47. J. Tritthart, Chloride binding in cement. II. The influence of the hydroxide concentration in the pore solution of hardened cement paste on chloride binding, Cem. Concr. Res. 19 (1989) 683-691.
48. A. Hidalgo, G. De Vera, M.A. Climent, C. Andrade, C. Alonso, Measurements of chloride activity coefficients in real portland cement paste pore solutions, J. Am. Ceram. Soc. 84 (2001) 3008-3012.
49. B. Elsener, L. Zimmermann, H. Böhni, Non destructive determination of the free chloride content in cement based materials, Mater. Corros. 54 (2003) 440-446.
50. S. Diamond, Effects of two danish flyashes on alkali contents of pore solutions of cement-flyash pastes, Cem. Concr. Res. 11 (1981) 383-394.
51. C.L. Page, Ø. Vennesland, Pore solution composition and chloride binding capacity of silica fume-cement pastes, Mater. Struct. 19 (1983) 19-25.
52. M. Kawamura, O.A. Kayyali, M.N. Haque, Effects of flyash on pore solution composition in calcium and sodium chloride-bearing mortars, Cem. Concr. Res. 18 (1988) 763-773.

53. J.A. Larbi, A.L.A. Fraay, J.M.J.M. Bijen, The chemistry of the pore fluid of silica fume-blended cement systems, Cem. Concr. Res. 20 (1990) 506-516.
54. J.L. García Calvo, A. Hidalgo, C. Alonso, L. Fernández Luco, Development of low-pH cementitious materials for HLRW repositories: Resistance against ground waters aggression, Cem. Concr. Res. 40 (2010) 1290-1297.
55. D.A. Hausmann, Steel corrosion in concrete. How does it occur?, Mater. Protection 6 (1967) 19-23.
56. C.L. Page, P. Lambert, P.R.W. Vassie, Investigations of reinforcement corrosion. 1. The pore electrolyte phase in chloride-contaminated concrete, Mater. Struct. 24 (1991) 243-252.
57. P. Lambert, C.L. Page, P.R.W. Vassie, Investigations of reinforcement corrosion. 2. Electrochemical monitoring of steel in chloride-contaminated concrete, Mater. Struct. 24 (1991) 351-358.
58. H. Justnes, A review of chloride binding in cementitious systems, Nordic Concrete Research Publication No. 21. 1/98 (1998) 48-63.
59. C.K. Larsen, Chloride binding in concrete, Dr. Ing. Thesis, Report No 1998:101, Norwegian University of Science and Technology, NTNU, 1998.
60. C. Arya, N.R. Buenfeld, J.B. Newman, Factors influencing chloride-binding in concrete, Cem. Concr. Res. 20 (1990) 291-300.
61. C.L. Page, N.R. Short, W.R. Holden, A reply to discussion by B.B. Hope, A. Ip and J.A. Page of the paper "the influence of different cements on chloride-induced corrosion of reinforcing steel", Cem. Conc. Res. 16 (1986) 977-979.
62. K. Tuutti, Corrosion of steel in concrete, Swedish Cement and Concrete Research Institute, 1982.
63. L.O. Nilsson, E. Poulsen, P. Sandberg, H.E. Sørensen, O. Klinghoffer, Chloride penetration into concrete - state of the art, HETEK report Nr. 53, 1996.
64. L.O. Nilsson, Models for chloride ingress into concrete - from Collepardi to today, Int. J. Modelling, Identification and Control 7 (2009) 129-134.
65. P. Mangat, B. Molloy, Prediction of long term chloride concentration in concrete, Mater. Struct. 27 (1994) 338-346.
66. M. Nokken, A. Boddy, R.D. Hooton, M.D.A. Thomas, Time dependent diffusion in concrete - three laboratory studies, Cem. Conc. Res. 36 (2006) 200-207.
67. S. Helland, R. Aarstein, M. Maage, In-field performance of north sea offshore platforms with regard to chloride resistance, Struct. Concr. 11 (2010) 15-24.
68. J. Gulikers, Considerations on the reliability of service life predictions using a probabilistic approach, J. Phys. IV 136 (2006) 233-241.
69. Model code for service life design, fib Bulletin No. 34, Lausanne, 2006.
70. DuraCrete Final Technical Report, "The European Union - Brite EuRam III, DuraCrete - Probabilistic performance based durability design of concrete structures", 2000.
71. O.E. Gjørv, Durability design of concrete structures in severe environments, Taylor & Francis, Abingdon, 2009.
72. F. Hunkeler, The resistivity of pore water solution - a decisive parameter of rebar corrosion and repair methods, Constr. Build. Mater. 10 (1996) 381-389.
73. D.A. Whiting, M.A. Nagi, Electrical resistivity of concrete - a literature review, Portland Cement Association, Skokie, Illinois, 2003.
74. A. Molina, C. Andrade, C. Alonso, J.A. González, Factores controlantes de la velocidad de corrosion de las armaduras embebidas en morteros de cemento, Rev. Téc. Ing., Univ. Zulia 8 (1985) 9-15. (in Spanish)
75. C. Alonso, C. Andrade, J.A. González, Relation between resistivity and corrosion rate of reinforcements in carbonated mortar made with several cement types, Cem. Concr. Res. 8 (1988) 687-698.
76. S. Feliu, J.A. González, S. Feliu (Jr), C. Andrade, Relationship between conductivity of concrete and corrosion of reinforcing bars, Br. Corros. J. 24 (1989) 195-198.
77. G.K. Glass, C.L. Page, N.R. Short, Factors affecting the corrosion rate of steel in carbonated mortars, Corros. Sci. 32 (1991) 1283-1294.
78. W. López, J.A. González, Influence of the degree of pore saturation on the resistivity of concrete and the corrosion rate of steel reinforcement, Cem. Concr. Res. 23 (1993) 368-376.
79. S. Fiore, R.B. Polder, R. Cigna, Evaluation of the concrete corrosivity by means of resistivity measurements, in: C.L. Page, P.B. Bamforth, J.W. Figg (Eds.), Proc. 4th Int. Symp. "Corrosion of

Reinforcement in Concrete Construction", Cambridge, UK, The Royal Society of Chemistry, 1996, pp. 273-282.
80. C. Andrade, C. Alonso, Corrosion rate monitoring in the laboratory and on-site, Constr. Build. Mater. 10 (1996) 315-328.
81. L. Bertolini, R.B. Polder, Concrete resistivity and reinforcement corrosion rate as a function of temperature and humidity of the environment, TNO report 97-BT-R0574, TNO Building and Construction Research, Delft, The Netherlands, 1997.
82. T. Liu, R.W. Weyers, Modeling the dynamic corrosion process in chloride contaminated concrete structures, Cem. Concr. Res. 28 (1998) 365-379.
83. W. Morris, A. Vico, M. Vazquez, S.R. de Sanchez, Corrosion of reinforcing steel evaluated by means of concrete resistivity measurements, Corros. Sci. 44 (2002) 81-99.
84. W. Morris, A. Vico, M. Vázquez, Chloride induced corrosion of reinforcing steel evaluated by concrete resistivity measurements, Electrochim. Acta 49 (2004) 4447-4453.
85. J. Gulikers, Theoretical considerations on the supposed linear relationship between concrete resistivity and corrosion rate of steel reinforcement, Mater. Corros. 56 (2005) 393-403.
86. M. Stern, A.L. Geary, Electrochemical polarization. I. A theoretical analysis of the shape of polarization curves, J. Electrochem. Soc. 104 (1957) 56-63.
87. C. Andrade, J.A. González, Quantitative measurements of corrosion rate of reinforcing steels embedded in concrete using polarization resistance measurements, Mater. Corros. 29 (1978) 515-519.
88. W. Oelßner, F. Berthold, U. Guth, The iR drop - well-known but often underestimated in electrochemical polarization measurements and corrosion testing, Mater. Corros. 57 (2006) 455-466.
89. C. Andrade, C. Alonso, J. Gulikers, R. Polder, R. Cigna, Ø. Vennesland, M. Salta, A. Raharinaivo, B. Elsener, Recommendation of RILEM TC 154-EMC: "Test methods for on-site corrosion rate measurement of steel reinforcement in concrete by means of the polarization resistance method", Mater. Struct. 37 (2004) 623-643.
90. P.V. Nygaard, Non-destructive electrochemical monitoring of reinforcement corrosion, ISBN 97-8877-877-2695, Department of Civil Engineering, Technical University of Denmark, DTU, 2008.
91. W.J. McCarter, R. Brousseau, The a.c. response of hardened cement paste, Cem. Concr. Res. 20 (1990) 891-900.
92. B. Elsener, H. Böhni, Corrosion of steel in mortar studied by impedance measurements, Mater. Sci. Forum 8 (1986) 363-372.
93. B.B. Hope, J.A. Page, A.K.C. Ip, Corrosion rates of steel in concrete, Cem. Concr. Res. 16 (1986) 771-781.
94. W.J. McCarter, G. Starrs, T.M. Chrisp, Electrical monitoring methods in cement science, in: J. Bensted, P. Barnes (Eds.), Structure and Performance of Cements, 2nd ed., Spon Press, Taylor & Francis, London, 2002, pp. 442-456.
95. R. Polder, C. Andrade, B. Elsener, Ø. Vennesland, J. Gulikers, R. Weidert, M. Raupach, RILEM TC 154-EMC: Electrochemical techniques for measuring metallic corrosion: "Test methods for on site measurement of resistivity of concrete". 33 (2000) 603-611.
96. J.-M. Østvik, C.K. Larsen, Ø. Vennesland, E.J. Sellevold, M.C. Andrade, Electrical resistivity of concrete, part I: Frequency dependence at various moisture contents and temperatures, in: J. Marchand, B. Bissonnette, R. Gagné, M. Jolin, F. Paradis (Eds.), 2nd Int. Symp. on Advances in Concrete through Science and Engineering, Quebec City, Canada, Rilem, 2006.
97. R.S. Barneyback, S. Diamond, Expression and analysis of pore fluids from hardened cement pastes and mortars, Cem. Concr. Res. 11 (1981) 279-285.
98. C. Arya, An assessment of four methods of determining the free chloride content of concrete, Mater. Struct. 23 (1990) 319-330.
99. Recommendation of RILEM TC 178-TMC: "Testing and modelling chloride penetration in concrete": Analysis of total chloride content in concrete., Mater. Struct. 35 (2002) 583-585.
100. ASTM C-1152, Standard test method for acid-soluble chloride in mortar and concrete, American Society for Testing and Materials.
101. SIA 162/2, Quantitative Bestimmung des Chloridgehalts von Beton, 2001, Schweizer Ingenieur- und Architektenverein. (in German)
102. M. Castellote, C. Andrade, Round-Robin test on chloride analysis in concrete - Part I: Analysis of total chloride content, Mater. Struct. 34 (2001) 532-556.

103. J. Goldstein, D.E. Newbury, D.C. Joy, C.E. Lyman, P. Echlin, E. Lifshin, L. Sawyer, J.R. Michael, Scanning Electron Microscopy and X-ray Microanalysis, 3rd ed, Kluwer Academic / Plenum Publishers, New York, 2003.
104. C.M. Hansson, T. Frølund, J.B. Markussen, The effect of chloride cation type on the corrosion of steel in concrete by chloride salts, Cem. Conc. Res. 15 (1985) 65-73.
105. A.K. Suryavanshi, J.D. Scantlebury, S.B. Lyon, Pore size distribution of OPC & SRPC mortars in presence of chlorides, Cem. Concr. Res. 25 (1995) 980-988.
106. P.G. de Viedma, M. Castellote, C. Andrade, Comparison between several methods for determining the depassivation threshold value for corrosion onset, J. Phys. IV 136 (2006) 79-88.
107. W. Breit, Critical corrosion inducing chloride content - state of the art and new investigation results, Verein Deutscher Zementwerke e.V., Verlag Bau+Technik, Düsseldorf, 2001.
108. L. Zimmermann, Korrosionsinitiierender Chloridgehalt von Stahl in Beton, Dissertation, ETH Nr. 13870, ETH Zürich, 2000. (in German)
109. P.V. Nygaard, M.R. Geiker, A method for measuring the chloride threshold level required to initiate reinforcement corrosion in concrete, Mater. Struct. 38 (2005) 489-494.
110. P. Schiessl, M. Raupach, Influence of concrete composition and microclimate on the critical chloride content in concrete, in: C.L. Page, K.W.J. Treadaway, P.B. Bamforth (Eds.), Proc. 3rd Int. Symp. "Corrosion of Reinforcement in Concrete", Wishaw, UK, Elsevier Applied Science, 1990, pp. 49-58.
111. K. Pettersson, Corrosion threshold value and corrosion rate in reinforced concrete, Swedish Cement and Concrete Research Institute, Stockholm, 1992.
112. P. Schiessl, W. Breit, Local repair measures at concrete structures damaged by reinforcement corrosion - aspects of durability, in: C.L. Page, P.B. Bamforth, J.W. Figg (Eds.), Proc. 4th Int. Symp. "Corrosion of Reinforcement in Concrete Construction", Cambridge, UK, The Royal Society of Chemistry, 1996, pp. 525-534.
113. P. Sandberg, Chloride initiated reinforcement corrosion in marine concrete, Dissertation (Report TVBM-1015), Lund Institute of Technology, Division of Building Materials, Lund University, 1998.
114. C. Alonso, C. Andrade, M. Castellote, P. Castro, Chloride threshold values to depassivate reinforcing bars embedded in a standardized OPC mortar, Cem. Concr. Res. 30 (2000) 1047-1055.
115. M. Moreno, W. Morris, M.G. Alvarez, G.S. Duffó, Corrosion of reinforcing steel in simulated concrete pore solutions: Effect of carbonation and chloride content, Corros. Sci. 46 (2004) 2681-2699.
116. M. Manera, Ø. Vennesland, L. Bertolini, Chloride threshold for rebar corrosion in concrete with addition of silica fume, Corros. Sci. 50 (2008) 554-560.

LIST OF PAPERS

This thesis includes the following ten appended papers. They are referred to by their Roman numbers.

I **Potentiometric determination of the chloride ion activity in cement based materials**

U. Angst, B. Elsener, C.K. Larsen, and Ø. Vennesland
Journal of Applied Electrochemistry 40 (2010) 561–573
Download from journal website: doi:10.1007/s10800-009-0029-6

II **Diffusion potentials as source of error in electrochemical measurements in concrete**

U. Angst, Ø. Vennesland, and R. Myrdal
Materials and Structures 42 (2009) 365–375
Download from journal website: doi:10.1617/s11527-008-9387-5

III **Detecting critical chloride content in concrete using embedded ion selective electrodes – effect of liquid junction and membrane potentials**

U. Angst and Ø. Vennesland
Materials and Corrosion 60 (2009) 638–643
Download from journal website: doi:10.1002/maco.200905280

IV **Diffusion potentials in porous mortar in a moisture state below saturation**

U. Angst, B. Elsener, R. Myrdal, and Ø. Vennesland
Electrochimica Acta 55 (2010) 8545–8555
Download from journal website: doi:10.1016/j.electacta.2010.07.085

V **Critical chloride content in reinforced concrete – A review**

U. Angst, B. Elsener, C.K. Larsen, and Ø. Vennesland
Cement and Concrete Research 39 (2009) 1122–1138
Download from journal website: doi:10.1016/j.cemconres.2009.08.006

VI **Chloride induced reinforcement corrosion: electrochemical monitoring of initiation stage and chloride threshold values**

U. Angst, B. Elsener, C.K. Larsen, and Ø. Vennesland
Corrosion Science 53 (2011) 1451–1464
Download from journal website: doi:10.1016/j.corsci.2011.01.025

VII Probabilistic considerations on the effect of specimen size on the critical chloride content in reinforced concrete

U. Angst, A. Rønnquist, B. Elsener, C.K. Larsen, and Ø. Vennesland
Corrosion Science 53 (2011) 177–187
Download from journal website: doi:10.1016/j.corsci.2010.09.017

VIII Influence of casting direction on chloride-induced rebar corrosion

U. Angst, B. Elsener, C.K. Larsen, and Ø. Vennesland
In: Proceedings of CONSEC'10. *Concrete under Severe Conditions, Environment and Loading, Vol. 1.* Eds: P. Castro-Borges et al., Taylor & Francis, 2010, pp. 359–366.
ISBN 978-0-415-59316-8.

IX Defects at the steel/concrete interface and their influence on chloride induced reinforcement corrosion

U. Angst, B. Elsener, C.K. Larsen, and Ø. Vennesland
Cement and Concrete Research (submitted)

X Chloride induced reinforcement corrosion: rate limiting step of early pitting corrosion

U. Angst, B. Elsener, C.K. Larsen, and Ø. Vennesland
Electrochimica Acta (in press)
Download from journal website: doi:10.1016/j.electacta.2011.04.124

Declaration of authorship for papers I–X

Ueli Angst planned and conducted the major part of the experiments, did the numerical simulations, evaluated the results, and wrote the appended papers. In general the co-authors contributed with constructive criticism that increased the scientific quality of the publications.

As specific additional contributions, Ø. Vennesland, C. K. Larsen, and B. Elsener were involved in planning the experiments for paper I (calibration of ISEs in solution and mortar) and in designing the specimens and the setup that formed a basis for papers VI, VIII, IX, and partly for paper X. During a stay at ETH Zurich in September 2010, B. Elsener gave helpful guidance for evaluation and discussion of the results in papers VI and X. Some of the ideas presented in paper VII, particularly the structural considerations, evolved from discussions with A. Rønnquist.

Ueli Angst performed the major part of the experimental work with exception of chemical analyses (all measurements of chloride content in concrete powder (SINTEF Building and Infrastructure, Trondheim); pore solution composition analysis (preBIO, Namsos) in paper IV), and scanning electron microscopy and X-ray microanalysis in papers I and IX (technical assistance by NTNU Trondheim and ETH Zurich).

OTHER PUBLICATIONS

In addition to papers I–X, the following publications resulted from the work carried out in the present PhD project. These publications are not appended to the present thesis.

Journal papers

- U. Angst. A discussion of the paper "Influence of surface charge on ingress of chloride ion in hardened pastes" by Y. Elakneswaran, T. Nawa, and K. Kurumisawa. *Materials and Structures* 44 (2011) 1–3.
  Download from journal website: doi:10.1617/s11527-010-9667-8

Book chapter

- M.C. Alonso, U. Angst, M. Sanchez, and K.Y. Ann. Onset of chloride induced reinforcement corrosion. In: Handbook of concrete durability. Ed: S.-H. Kim, K.Y. Ann. Middleton Publishing Inc. (2010), ISBN 351-2010-000013, pp. 1–48.

Conference papers

- U. Angst, B. Elsener, C.K. Larsen, and Ø. Vennesland. Considerations on the effect of sample size for the critical chloride content in concrete. In: Service Life Design for Infrastructure, Proc. 2nd Int. Symp., Delft, The Netherlands. Volume 1. Ed: K. van Breugel et al. RILEM Publications S.A.R.L., 2010, pp. 569–576.
  ISBN 978-2-35158-113-1.

- U. Angst, C.K. Larsen, Ø. Vennesland, and B. Elsener. Monitoring the chloride concentration in the concrete pore solution by means of direct potentiometry. In: Concrete Solutions, Proc. Int. Conf. on Concrete Solutions, Padua, Italy. CRC Press/Balkema, The Netherlands, 2009, p. 401.
  ISBN 978-0-415-55082-6.

- U. Angst and Ø. Vennesland. Critical chloride content in reinforced concrete – state of the art. In: Concrete Repair, Rehabilitation and Retrofitting II. Proc. 2nd Int. Conf. on Concrete Repair, Rehabilitation and Retrofitting (ICCRRR), Cape Town, South Africa. CRC Press/Balkema, The Netherlands, 2008, p. 149.
  ISBN 978-0-415-46850-3.

- U. Angst, Ø. Vennesland, C.K. Larsen, and B. Elsener. Critical chloride content for corrosion in reinforced concrete. In: Nordic Concrete Research, Proceedings 20th NCR meeting, Bålsta, Sweden. Norsk Betongforening, Oslo, 2008, p. 52.
  ISBN 978-82-8208-007-1.